32

ER ID# 57571

Broxton et al. in review

STRATIGRAPHY, MINERALOGY AND CHEMISTRY OF BEDROCK TUFFS AT MESITA DEL BUEY, LOS ALAMOS NATIONAL LABORATORY, NEW MEXICO

by

D. E. Broxton, C. LaDelfe, S. J. Chipera, and E. C. Kluk

Geology/Geochemistry Group
Los Alamos National Laboratory

ABSTRACT

Geologic investigations were conducted at Mesita del Buey to develop a geologic conceptual model for the site, to evaluate potential groundwater pathways and processes, and provide geologic data for performance assessment of MDA G. Six stratigraphic sections were measured in bedrock units exposed in Pajarito Canyon and Canada del Buey to provide information about the tuffs that underlie Mesita del Buey. Selected samples from these stratigraphic sections were analyzed by x-ray diffraction for mineralogy, x-ray fluorescence for chemistry, and microscopy for petrography. These investigations were conducted in support of the Environmental Restoration Project at Los Alamos National Laboratory.

Exposed bedrock in the vicinity of Mesita del Buey consists of fluvial sediments of the Cerro Toledo interval which are overlain by pyroclastic rocks of the Tshirege Member of the Bandelier Tuff. The Tshirege Member, a compound cooling unit, is further subdivided based on welding and alteration characteristics. In ascending order, the Tshirege Member consists of: 1) the Tsankawi Pumice Bed; 2) unit 1g, nonwelded glassy ignimbrite; 3) unit 1v, nonwelded devitrified and vapor phase altered ignimbrite; and 4) unit 2, resistant, cliff-forming ignimbrite that forms the mesa's caprock.

Unit 1g is relatively unaltered and contains abundant volcanic glass. Units 1v and 2 are devitrified and vapor-phase altered, and their mineralogy is dominated by alkali feldspar (~60% by weight) and by combinations of three silica polymorphs (tridymite, quartz, and cristobalite). The abundances of the silica minerals in units 1v and 2 vary as a function of stratigraphic position as well as distance from the source caldera. Tridymite abundances are greatest in unit 2 and in the upper part of unit 1v in the westermost part of Mesita del Buey. Further east, tridymite abundances decrease overall, and significant tridymite concentrations are restricted to unit 2. Cristobalite abundances vary inversely with respect to tridymite. High tridymite abundances in unit 2 suggest that post-emplacement vapor-phase activity was greater in the upper tuff units.

Received by ER-RPF
APR 2 0 1998

13519

The decrease in tridymite abundances coupled with the thinning of units suggest that vapor phase activity decreased eastward in the distal parts of these tuffs.

The Tshirege Member at Mesita del Buey is a high-silica rhyolite (77% SiO_2). Major element abundances are relatively constant, but some trace element abundances vary with stratigraphic height. The most pronounced chemical changes take place across the unit 1v/unit 2 contact in the eastern part of the study area. However, futher to the west, there is a compositional continuum across the same contact, probably reflecting a more complete depositional sequence for the Tshirege Member in that area.

INTRODUCTION

This study was conducted as part of site characterization activities for the Environmental Restoration (ER) Project at Technical Area 54 (TA-54). TA-54 is located on Mesita del Buey, the site of the Laboratory's solid and liquid hazardous waste disposal sites MDA G and MDA L (Fig. 1). This study describes the bedrock geology of Mesita del Buey and its adjacent canyons. It was conducted to provide information for a geological conceptual model for the site, to evaluate potential groundwater pathways and processes, and to provide geological data specifically required for performance assessment. In addition, the geologic information contained herein supports the design and construction of waste pits, monitoring systems, and support facilities. A report that includes subsurface geology and hydrologic setting was compiled for a radiological performance assessment of the site (Krier et al., 1995).

Stratigraphy is a important component of site wide studies of geology of the Pajarito Plateau for the ER Project. These site wide studies are a requirement of the HSWA Module VIII of the Laboratory's RCRA Part B operating permit. Section P, Task III, Facility Investigation, Subtask A.1 of the HSWA module, requires a program to evaluate site hydrogeological conditions, including geologic and hydrogeological characteristics affecting groundwater flow beneath the facility. The permit specifies that the depth, thickness, and lateral extent of hydrogeological units which may be migration pathways be identified based on field studies, core studies, structural geology, and cross sections. This study, coupled with previous and on-going investigations, address these requirements of the HSWA permit.

Six stratigraphic sections were measured for bedrock units of the Bandelier Tuff exposed on the north wall of Pajarito Canyon and of Canada del Buey and its tributaries. The locations of these stratigraphic sections are shown in Fig. 1, and summary figures for each section are provided in Appendix A. The stratigraphic sections form three north-south pairs that were used to construct a fence diagram of bedrock units at Mesita del Buey. The fence diagram provides information about the distribution and thicknesses of tuffs that underlie Mesita del Buey.

A companion report by Reneau et al. (in review) presents the results of a detailed survey that maps the distribution and thickness of surge deposits in the basal part of unit 2. These surge deposits are important because they may provide preferential pathways for the migration of

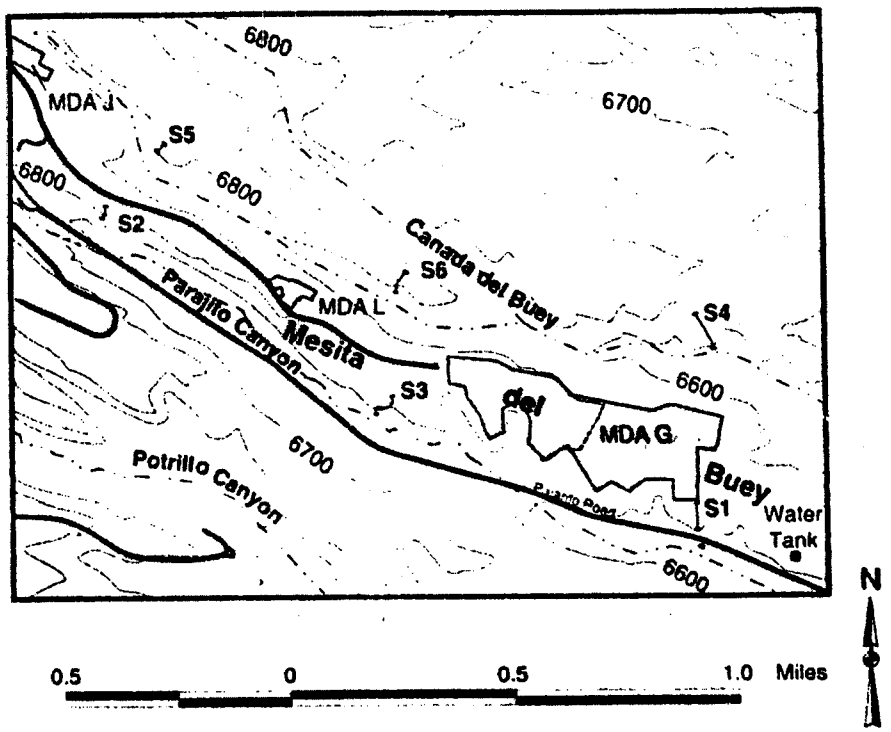

Fig. 1 Map of Mesita del Buey showing locations of stratigraphic sections S1 through S6.

moisture and contaminants at MDAs G and L. The report by Reneau et al. also summarizes information about faults found on the south side of Mesita del Buey during the surge survey. A bedrock geologic map is being prepared for the site, and it will be presented in a later report. The geologic map and the stratigraphic data presented in this report contribute to conceptual models for the site and provide a geologic framework for understanding the potential for contaminant migration at Mesita del Buey.

METHODS

Field work was performed using the procedure Characterization of Lithologic Variations within the Rock Outcrops of a Volcanic Field (LANL-ER-SOP-03.07). Field observations in each stratigraphic section generally included descriptions of rock type, unit thickness, type and degree of alteration, welding and compaction, phenocryst assemblage and abundance, color on fresh and weathered surfaces, pumice size and abundance, and weathering characteristics. Bedding characteristics, fractures and their filling materials, and lithic assemblage, size, and abundance were also noted. Bulk-tuff samples were collected at a nominal vertical spacing of 5 m or at major changes in lithology. Metal tags mark sample sites in the field. Vertical control was maintained by Jacob staff and Abney level in the field, and locations and elevations were estimated from maps. Some of the sample sites whose locations were close to a surge bed survey line (see accompanying report) were surveyed by infrared theodolite (Table I).

Major and trace elements were analyzed in samples using an automated Rigaku wavelength-dispersive X-ray fluorescence (XRF) spectrometer. Samples were prepared by crushing and homogenizing 15-20 g of the sample in a shatterbox in accordance with Yucca Mountain Project procedure LANL-EES-DP-130 (Geologic Sample Preparation). Sample splits were heated at 110°C for 24 hrs, and then 4-g splits were fused at 1100°C with 8 g of lithium metaborate/lithium tetraborate flux. Elemental concentrations were calculated by comparing X-ray intensities for the samples to those for 21 standards of known composition. A fundamental parameters program was used for matrix corrections (Criss, 1980) in accordance with Yucca Mountain Project procedure LANL-EES-DP-111.

The mineralogy of the tuffs was determined by x-ray diffraction (XRD) for 38 samples collected from stratigraphic sections 1, 2, 3, 5, and 6. Samples were first powdered in a tungsten-carbide shatter box and then mixed with an internal standard of 1 µm metallurgical grade Al_2O_3 (corundum) powder in a ratio of 80% sample to 20% internal standard by weight. The samples were then ground under acetone in an automatic Brinkmann-Retsch mill fitted with an agate mortar and pestle to produce an average particle size of less than 5 µm. This fine particle size is necessary to ensure adequate particle statistics and to minimize primary extinction (Klug and Alexander, 1974, pp. 365-367). Particle size distributions have been verified using a Horiba CAPA-500 centrifugal particle size distribution analyzer calibrated with Duke Scientific glass microsphere standards. X-ray diffraction (XRD) data were collected on a Siemens D-500 theta-theta diffractometer using copper-Ka radiation, incident- and diffracted-beam Soller slits, and a Kevex solid-state (SiLi) detector. Data were typically collected from 2.0 to 50.0° 2θ using a 0.02° step size and at least two seconds per step. Quantitative analyses employed the internal standard or "matrix-flushing" method of Chung (1974a,b). Details for analysis can be found in Bish and Chipera (1988; 1989). In addition, the following Yucca Mountain Project procedures were used for sample preparation and analysis of XRD samples: LANL-EES-DP-130 (Geologic Sample Preparation), LANL-EES-DP-56 (Brinkmann Automated Grinder Procedure), LANL-EES-DP-16 (Siemens X-Ray Diffraction Procedure), and LANL-EES-DP-116 (Quantitative X-Ray Diffraction Data Reduction Procedure). Yucca Mountain Project quality assurance requirements are comparable in rigor to those used by the Los Alamos Environmental Restoration Program.

Thin-section were prepared for 19 samples to describe the textures and alteration features of the tuffs. These samples are representative of the tuffs in stratigraphic sections 1, 2, and 4. The thin sections were prepared according to Yucca Mountain Project procedure LANL-EES-DP-130 (Geologic Sample Preparation) and petrographic observations were made using procedure LANL-ER-SOP-03.04 (Petrography).

RESULTS AND DISCUSSION

Stratigraphy and Lithology

The Bandelier Tuff is subdivided into two genetically related members, each with a basal pumice fall overlain by a petrologically related succession of ash flows (Griggs, 1964, Bailey et al., 1969, Smith et al., 1970). The lower member is designated the Otowi Member and was erupted at 1.613 ± 0.011 Ma (Izett and Obradovich, 1994) from a caldera source coincident

TABLE I.

LOCATIONS OF SAMPLES COLLECTED IN STRATIGRAPHIC SECTIONS AT MESITA DEL BUEY, LOS ALAMOS, NEW MEXICO[1]

Sample Number	Stratigraphic Unit [2]	Location ID	Coordinates North (ft)	Coordinates East (ft)	Elevation (ft)	Location Method [3]
Stratigraphic Section 1						
OU-1148-STRAT1-1	Qbt-1v	54-6900	1756563.9	1644778.9	6584.8	S
OU-1148-STRAT1-2	Qbt-1v	54-6901	1756572.2	1644776.0	6591.9	S
OU-1148-STRAT1-3	Qbt-1v	54-6902	1756575.9	1644779.9	6595.9	S
OU-1148-STRAT1-4	Qbt-1v	54-6903	1756594.8	1644788.9	6607.9	S
OU-1148-STRAT1-5	Qbt-1v	54-6904	1756597.7	1644787.5	6609.1	S
OU-1148-STRAT1-6	surge	54-6905	1756598.9	1644801.4	6610.0	S
OU-1148-STRAT1-7	Qbt-2	54-6906	1756599.5	1644803.3	6617.0	S
OU-1148-STRAT1-8	Qbt-2	54-6907	1756608.2	1644801.0	6630.0	S
OU-1148-STRAT1-9	Qbt-2	54-6908	1756833.9	1644805.9	6648.6	S
Stratigraphic Section 2						
OU-1148-STRAT2-1	Qbt-1v	54-6909	1760362.7	1637554.2	6713.2	S
OU-1148-STRAT2-2	Qbt-1v	54-6910	1760386.1	1637611.8	6730.8	S
OU-1148-STRAT2-3	Qbt-1v	54-6911	1760413.7	1637604.9	6751.2	S
OU-1148-STRAT2-4	Qbt-1v	54-6912	1760425.2	1637615.9	6767.2	S
OU-1148-STRAT2-5	Qbt-1v	54-6913	1760446.1	1637620.6	6784.0	S
OU-1148-STRAT2-6	Qbt-2	54-6914	1760461.5	1637611.7	6800.0	S
OU-1148-STRAT2-7	Qbt-2	54-6915	1760479.9	1637606.0	6826.2	S
OU-1148-STRAT2-8	Qbt-2	54-6916	1760515.0	1637645.0	6838.0	E
Stratigraphic Section 3						
OU-1148-STRAT3-1	Qbt-1v	54-6917	1757957.0	1640899.0	6649.0	E
OU-1148-STRAT3-2	Qbt-1v	54-6918	1757992.0	1640907.0	6666.9	S
OU-1148-STRAT3-3	Qbt-1v	54-6919	1758013.0	1640907.0	6683.0	E
OU-1148-STRAT3-4	Qbt-1v	54-6920	1758079.0	1641105.0	6703.3	S
OU-1148-STRAT3-5	Qbt-1v	54-6921	1758092.0	1641116.0	6715.2	S
OU-1148-STRAT3-6	Qbt-2	54-6922	1758101.0	1641113.0	6718.4	S
OU-1148-STRAT3-7	Qbt-2	54-6923	1758147.0	1641101.0	6733.9	S
Stratigraphic Section 4						
OU-1148-STRAT4-1	Qct	54-6924	1758721.0	1645056.0	6574.0	E
OU-1148-STRAT4-2A	Qbt-t	54-6925	1758740.0	1645006.0	6576.0	E
OU-1148-STRAT4-2B	Qbt-t	54-6926	1758740.0	1645006.0	6576.0	E
OU-1148-STRAT4-3	Qbt-1g	54-6927	1758813.0	1645022.0	6602.0	E
Stratigraphic Section 5						
OU-1148-STRAT5-1	Qbt-1v	54-6928	1761099.0	1638205.0	6749.0	E
OU-1148-STRAT5-2	Qbt-1v	54-6929	1761124.0	1638223.0	6765.0	E
OU-1148-STRAT5-3	Qbt-1v	54-6930	1761160.0	1638253.0	6781.0	E
OU-1148-STRAT5-4	Qbt-1v	54-6931	1761192.0	1638243.0	6797.0	E
OU-1148-STRAT5-5	Qbt-1v	54-6932	1761214.0	1638263.0	6814.0	E
OU-1148-STRAT5-6	Qbt-2	54-6933	1761226.0	1638271.0	6830.0	E
OU-1148-STRAT5-7	Qbt-2	54-6934	1761233.0	1638305.0	6848.0	E
Stratigraphic Section 6						
OU-1148-STRAT6-1	Qbt-1v	54-6935	1759453.0	1641161.0	6664.0	E
OU-1148-STRAT6-2	Qbt-1v	54-6936	1759497.0	1641168.0	6680.0	E
OU-1148-STRAT6-3	Qbt-1v	54-6937	1759549.0	1641180.0	6697.0	E
OU-1148-STRAT6-4	Qbt-1v	54-6938	1759571.0	1641185.0	6719.0	E
OU-1148-STRAT6-5	Qbt-2	54-6939	1759590.0	1641210.0	6734.0	E
OU-1148-STRAT6-6	Qbt-2	54-6940	1759598.0	1641209.0	6750.0	E
OU-1148-STRAT6-7	Qbt-2	54-6941	1759689.0	1641278.0	6768.0	E

[1] *Locations listed as NAD83 State Plane Coordinates.*
[2] *Strat. Unit - Qbt-t = Tsankawi Pumice Bed; Qbt-1g = Tshirege unit 1, lower glassy part; Qbt-1v = Tshirege unit 1, upper vapor-phase altered and devitrified part; Qbt 2 = Tshirege unit 2*
[3] *S = Sample locations surveyed by J. Carney, D. Broxton, and C. LaDelfe, 1993. E = Location estimated from maps using adjacent surveyed samples and from Jacob staff traverse.*

with the younger Valles caldera (Goff et al., 1984; Self et al., 1986). The upper member is the Tshirege Member, and it was erupted from the Valles caldera (Smith and Bailey, 1966; Smith et al., 1970) at 1.223 ±0.018 Ma (Izett and Obradovich, 1994).

Otowi Member

The Otowi Member is not exposed at Mesita del Buey, but it has been recognized in the subsurface at boreholes 54-1004 and 54-1015. It is 33 m thick in borehole 54-1015, including the 3.3 m-thick Guaje Pumice Bed (John Marin, ERM; personal communication). The upper 13.8 m of the unit was penetrated in borehole 54-1004 where it is a massive, nonwelded, pumice-rich, vitric ignimbrite (Caporuscio, 1994). Gray to light yellow brown pumices make up about 20% of the tuff. The massive nature of the deposit is interrupted by sporadic pumice swarms (~30% pumices) that occur at discrete intervals up to 0.6 m thick. Pumices are fully inflated and the delicate tube structures of vesicles are preserved. The pumices are supported by a tan matrix consisting of glass shards, phenocrysts, perlite clasts, and broken pumice fragments. The Otowi Member contains 7 to 9% phenocrysts of quartz and sanidine and minor clinopyroxene (Broxton et al, 1995a). Quartz and sanidine phenocrysts are typically 0.5 mm to 2 mm in diameter. Accessory minerals include magnetite, zircon, and chevkinite.

The Otowi Member probably has uniform hydrologic properties because of its massive nonwelded nature. The mean porosity for the unit is 47±5% and the mean bulk density is 1.25±0.2 g/cm^3 (Rogers and Gallaher, 1995). In borehole CDBM-1, located in upper Canada del Buey, hydrologic properties of the unit vary little with depth (Rogers and Gallaher, 1995).

Cerro Toledo Interval

The Otowi Member is overlain by epiclastic sediments and tephras informally designated the Cerro Toledo interval (Broxton et al., 1995a; Goff, 1995). A small exposure of the Cerro Toledo interval crops out at stream level in Canada del Buey, north of MDA G. The Cerro Toledo interval was encountered in the subsurface by six boreholes (54-1001 through 54-1006) at MDA L (Caporuscio, 1994) as well as in borehole 54-1015 (John Marin, ERM; personal communication). The Cerro Toledo interval is 12-17 m thick in boreholes 54-1004, 54-1006, and 54-1015.

The Cerro Toledo interval is a complex succession of volcaniclastic sediments and primary tephras (?). In general, the unit consists of two distinct types of deposits: (1) tuffaceous deposits composed of sandstones, siltstones, ash beds, and pumice falls and (2) sand, gravel, cobble and boulder deposits made up of dacitic detritus derived from the Tschicoma Formation (Broxton et al., 1995a; Goff, 1995). At Mesita del Buey, the Cerro Toledo interval includes both tuffaceous and dacitic deposits (Caporuscio, 1994). The middle and upper part of the unit consists of reworked tuffaceous sands intercalated with possible primary ash- and pumice-fall deposits (Caporuscio, 1994). A cobble-rich zone was encountered in the lower part of the unit by six boreholes (54-1001 to 54-1006) in the vicinity of MDA L. The cobble-rich zone is up to [illegible] m thick in borehole 54-1004, and consists of dacitic clasts (75% by vol.) in a crystal-, ash-, and pumice-rich matrix (Caporuscio, 1994).

Cerro Toledo deposits are well stratified and contain numerous thin depositional subunits characterized by a variety of lithologies. In addition, tuffs at top of the unit are oxidized and clay-rich indicating they are probably modified by soil development. The lithologic heterogeneity of the Cerro Toledo interval results in variable hydraulic properties for these deposits.

(Rogers and Gallaher, 1995). The juxtaposition of beds with contrasting hydraulic properties may result in capillary and permeability barriers at the contacts of beds and cause groundwater and gases to divert laterally.

Tshirege Member

The Tshirege Member of the Bandelier Tuff is divided into mappable subunits which are described separately because of their distinct physical properties. This study follows the stratigraphic nomenclature of Broxton and Reneau (1995). A correlation chart showing Tshirege nomenclature used by earlier workers is provided for the convenience of readers comparing this work with older reports (Fig. 2). Only the Tsankawi Pumice Bed and units 1 and 2 of the Tshirege Member are present at Mesita del Buey. Unit 3, which crops out just west of Mesita del Buey, has been stripped from this area by erosion, and unit 4 was probably never deposited this far east on the Pajarito Plateau.

The Tshirege Member is a multiple-flow ash-flow sheet that forms prominent cliffs and benches at Mesita del Buey and surrounding mesas. It is 70 m thick beneath the mesa in the vicinity of MDA L and thins to approximately 45 m thick in the vicinity of MDA G. Eastward thinning reflects the onlap of the Tshirege Member onto a paleotopographic high consisting of basalt

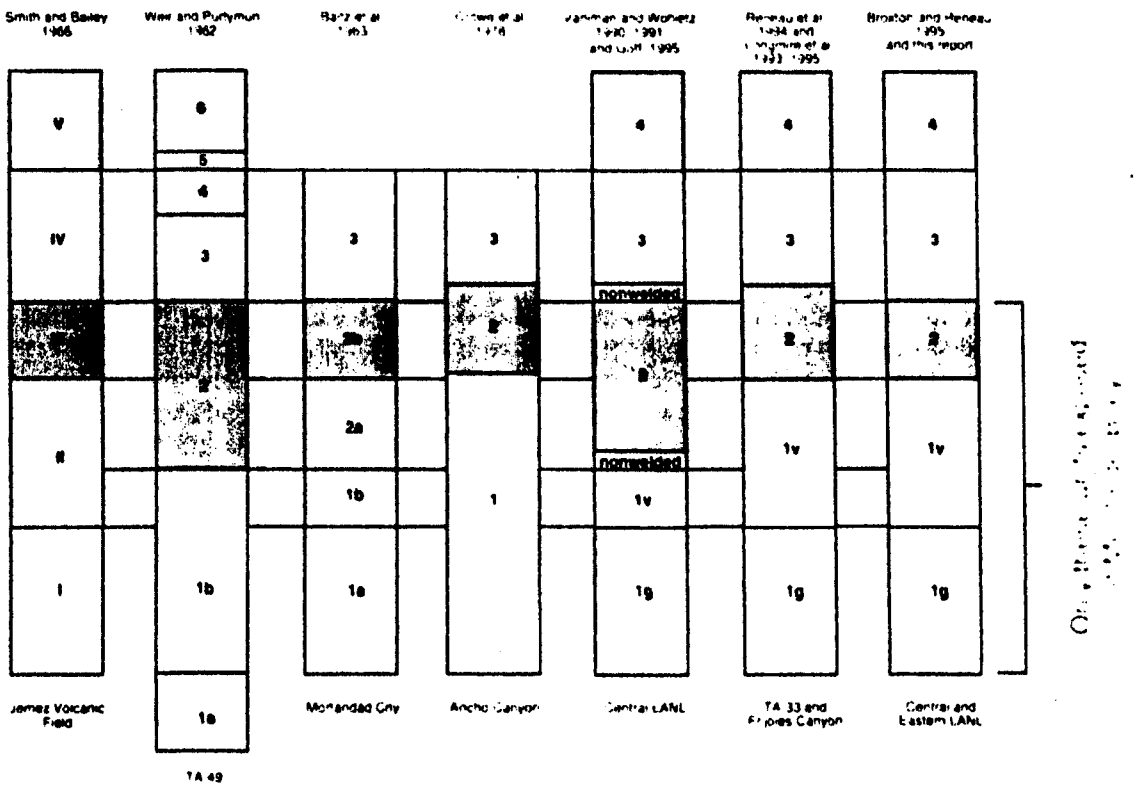

Fig. 2 Correlation chart showing rock unit names applied to the Bandelier Tuff by previous investigators

lava flows and vents in the vicinity of White Rock. Thus the Tshirege Member overlies the Cerro Toledo interval and the Otowi Member at MDA L but directly overlies basalt at White Rock.

Tsankawi Pumice Bed The Tsankawi Pumice Bed is the basal pumice fall of the Tshirege Member. It crops out on the north side of the stream channel in Canada del Buey, north of MDA G, where it is 22 cm to 50 cm thick.

The Tsankawi Pumice Bed consists of two light gray pumice fall deposits separated by a 1 cm-thick coarse ash bed. The lower pumice fall is four to five times thicker than the upper pumice fall. The pumice falls consist of angular to subangular clast-supported pumices 1 to 3 cm in diameter. Pumices are typically fibrous with a vitreous luster. The matrix consist largely of 1-2 mm felsic phenocrysts and broken pumice fragments. The volcanic glass in the pumices and matrix material is abundant and fresh, indicating these tuffs have undergone little diagenetic alteration since their deposition.

Pumices in the Tsankawi Pumice Bed are mostly rhyolitic in composition, but there is also a small (<5 %) population of medium-gray, dense, finely-vesiculated dacitic hornblende-bearing pumice (Table 1). These hornblende-bearing pumices are a diagnostic feature of the Tsankawi Pumice Bed and of overlying ash-flow units (Bailey et al., 1969).

Unit 1 Unit 1 is a thick succession of ash-flow tuffs that is characterized by lack of welding, despite its relatively thick accumulation in some areas. The unit is further divided into a lower glassy tuff (1g) and an upper devitrified and vapor-phase altered tuff (1v). Unit 1g is exposed near the canyon floor in the eastern part of Canada del Buey where it forms low rounded cliffs. Except for a small outcrop east of MDA G, Pajarito Canyon is not deep enough to expose unit 1g. Unit 1v is exposed in both Canada del Buey and Pajarito Canyon.

Unit 1g is a massive nonwelded vitric ignimbrite consisting of gray to tan vitreous pumice supported by a matrix of coarse ash, shards, pumice fragments. Phenocrysts are abundant (12-16%) and consist mostly of 1-2 mm quartz and sanidine (Broxton et al., 1995a). The base of the unit is a distinctive light-gray to white, nonconsolidated, massive, and ash-rich tuff. It grades upwards into light orange partially-consolidated pumice-rich ignimbrite. In this upper part, pumices are commonly 3 to 9 cm in diameter and make up 30 to 40% of the tuff. The matrix is pale orange in the upper part of unit 1g and becomes dark orange near the top of the unit.

In outcrop, the top of unit 1g is a resistant cliff-forming tuff, the top of which forms a bench that is several meters wide locally. The bench marks the base of the vapor-phase notch, a thin, horizontal zone of preferential weathering that marks the transition from the glassy tuffs of unit 1g to the crystallized tuffs of unit 1v. The contact is gradational over 0.3 to 1 m and is arbitrarily selected as the first appearance of volcanic glass going down section. Crystallization of volcanic glass in unit 1v indicates that (1) tuffs became hotter as eruption of unit 1 proceeded or (2) a combination of outgassing from lower tuffs and effective heat retention by a thick tuff sequence promoted slow cooling and crystallization in the upper of the unit.

Unit 1v forms a combination of cliff-like and sloping outcrops that separates the resistant bench at the top of unit 1g from the near-vertical cliff of unit 2. The basal part of unit 1v is a resistant orange-brown tuff that overlies the bench on top of unit 1g. This basal part has a

"colonnade" appearance due to the presence of abundant vertical fractures that serve as failure planes for rock falls, resulting in smooth dihedral surfaces on cliff faces. The colonnade tuff is overlain by slope-forming tuffs, hereafter referred to as upper unit 1v (Fig. 3). Upper unit 1v tuffs are relatively thick in the western part of Mesita del Buey, but thin significantly eastward (Fig. 3).

The colonnade tuff forms a cliff 6 m high near MDA L and 2-3 m high near MDA G. These tuffs may be slightly welded, although pumice relicts show no discernible compaction at the hand specimen scale. The colonnade tuff consists of soft, chocolate-brown to dark purple-gray pumice relicts supported by a pinkish-white to light-gray ashy matrix. Pumice relicts typically make up 30 to 50% of the rock and are 0.2 cm to 6 cm in diameter. Weathered tuff surfaces are pockmarked because of the selective weathering of soft pumices from the enclosing, more-resistant matrix. Broxton et al. (1995a) recommended treating the colonnade tuff as a separate hydrogeological unit because of its distinctive lithologic properties. The colon-

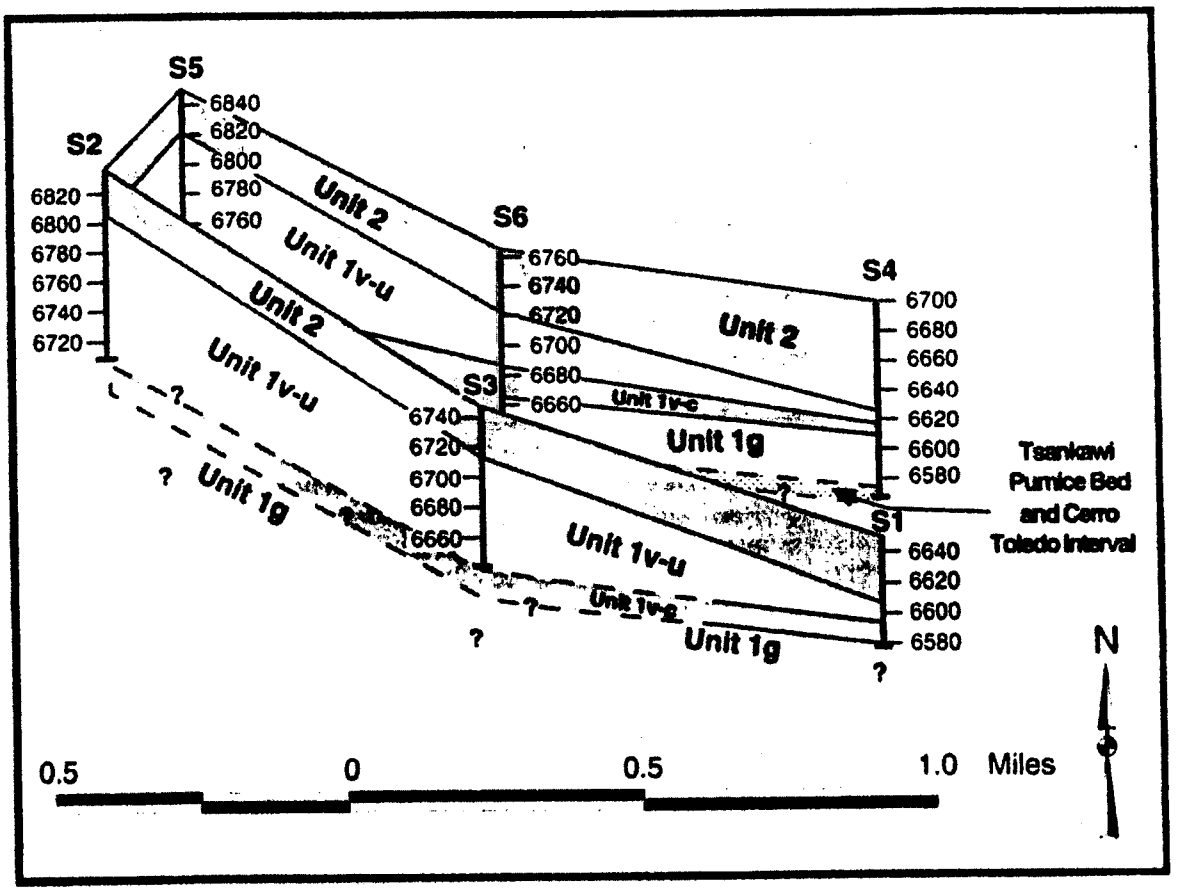

Fig. 3 Fence diagram of Mesita del Buey showing the distribution of bedrock tuff units in the Tshirege Member. The near face of the fence diagram represents data for stratigraphic sections on the north wall of Pajarito Canyon and the far face represents data for the north wall of Canada del Buey. Unit 1V-c is the lower "colonnade" part of unit 1v, and unit 1v-u is upper slope-forming part of unit 1v. See text for details. Note the thinning of unit 1v eastwards, particularly for unit 1v-u.

nade tuff has lower saturated and unsaturated hydraulic conductivities than slope-forming tuffs in the upper part of unit 1v (Turin et al., 1994). Fractures are more abundant in colonnade tuff relative to the glassy tuffs in unit 1g. Near-vertical fractures of the colonnade tuff typically die out at the boundary with unit 1g, although a few fractures persist across this lithologic contact. Fractures are open and fracture walls are commonly free of fracture-lining minerals.

Upper unit 1v forms a distinctive grayish-white band of outcrops sandwiched between the darker colored outcrops of the colonnade tuff and unit 2. In places, these tuffs form step-like outcrops which probably reflect slight variations in the amount of compaction of the tuffs (Fig. 4). However, outcrop weathering patterns probably are also affected by variations in the abundances of pumice relicts. Tuffs with abundant pumice relicts tend to erode more easily and form sloping outcrops whereas tuffs poor in pumice relicts are somewhat more resistant to erosion and form more resistant outcrops.

Upper unit 1v tuffs consist of soft pumice relicts supported by a pinkish-white to light-gray ashy matrix. Pumice contents are highly variable both vertically and laterally. Pumice relicts typically make up 10 to 30% of the tuff and are commonly 1-4 cm in diameter. These relicts are chocolate-brown and have good preservation of delicate vesicle structures in the lower part of upper unit 1v. In the upper part of this tuff sequence, pumice relicts are commonly brown-gray to medium-gray and relict pumice structures are relatively poorly preserved because of post-emplacement devitrification and vapor-phase alteration.

In some exposures, upper unit 1v has a stratified appearance due to the presence of horizontal zones of pumice accumulation. These zones of pumice accumulation are especially prominent near the top of the unit and may be preferential pathways for moisture and vapor movement because of their high porosity. Pumice relicts make up 30-50% of these tuffs and are 4-15 cm in diameter. In some cases the pumice accumulations occur at the tops of individual ash flows and represent the rafting of pumices to the tops of flows during emplacement. In other cases, entire ash flow depositional units are pumice-rich throughout and probably represent the distal parts of flow units that lost much of their fine ash during emplacement.

Unit 1v thins eastward from 27-30 m thick in the vicinity of MDA L to 4-8 m thick near the eastern end of MDA G (Fig. 3). Unit 1v is absent in outcrops just west of the visitor center in White Rock, and unit 2 directly overlies unit 1g (compare Figs. 4 and 5). The pinch out of unit 1v eastward may be due in part to the onlap of the Tshirege Member onto the basaltic highland in the vicinity of White Rock. However, lower units such as unit 1g also should pinch out against the basaltic highland if depositional onlap onto a paleohigh was the only factor controlling the distribution of these tuffs. Alternative hypotheses for the eastward thinning of unit 1v include (1) decreasing devitrification and vapor-phase alteration in the upper parts of unit 1 because of the loss of heat and gases towards its distal edge and (2) non-deposition of the upper, hotter ash flows of unit 1 in the eastern part of Mesita del Buey because of shorter runouts of its constituent ash flows relative to underlying and overlying tuff units.

The first hypothesis is supported by proximity of Mesita del Buey to the distal edge of unit 1. Crystallization of volcanic glass following emplacement requires high initial temperatures, slow cooling (promoted by the insulating effects of thick tuff deposits), and fluxing of volcanic gases (Smith, 1960). However, depositional thinning in the distal parts of ash-flow sheets promotes rapid cooling of the tuffs and tends to inhibit the crystallization of volcanic glass

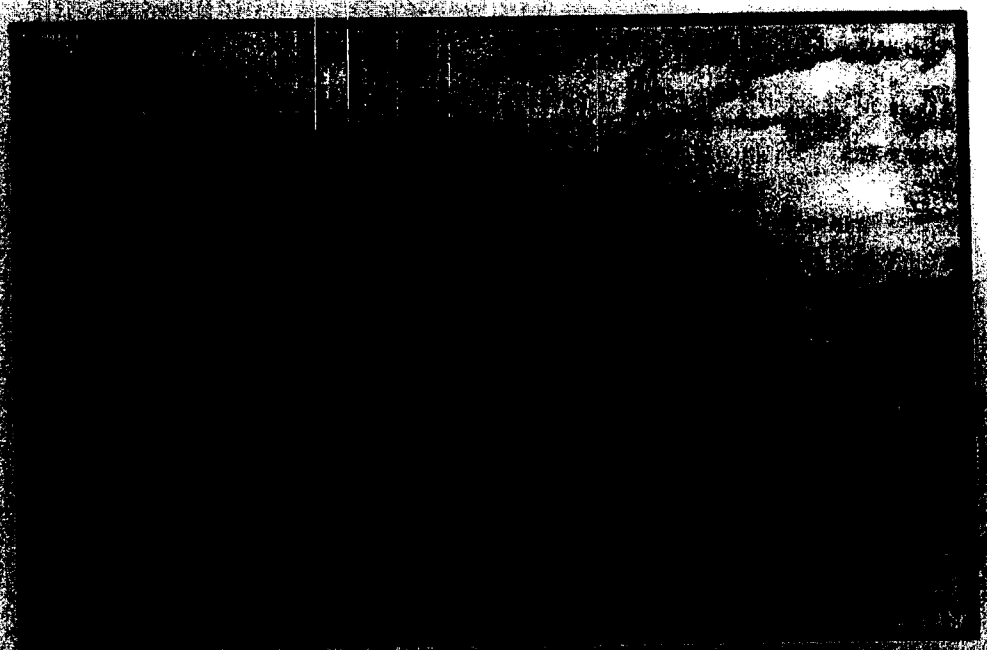

Fig. 4 South wall of [illegible] unit 1v. Yellowish less resistant tuffs of unit 1v. The [illegible] in unit 1v are due to slight variations in compaction and differential erosion of alternating pumice-rich and pumice-poor tuffs. Thin surge deposits occur at the base of the unit 2 cliff.

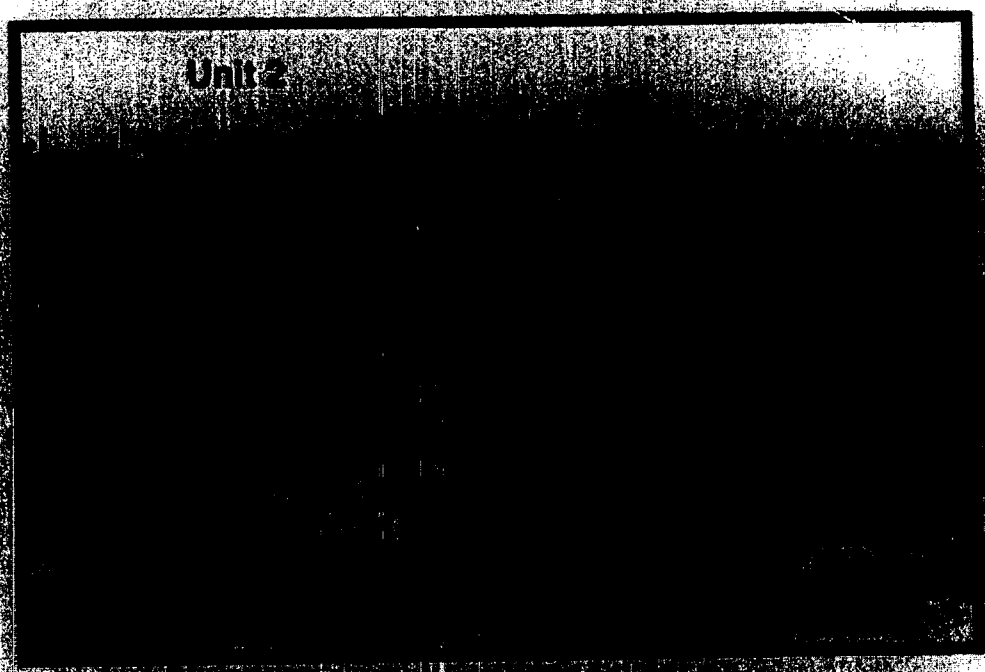

Fig. 5 East end of [illegible] the Bluff, just west of the visitor center in White Rock. Tshirege unit 2 directly overlies unit 1g on the right side of the photograph. A thin wedge of unit 1v occurs between units 2 and 1g on the left side of the photograph.

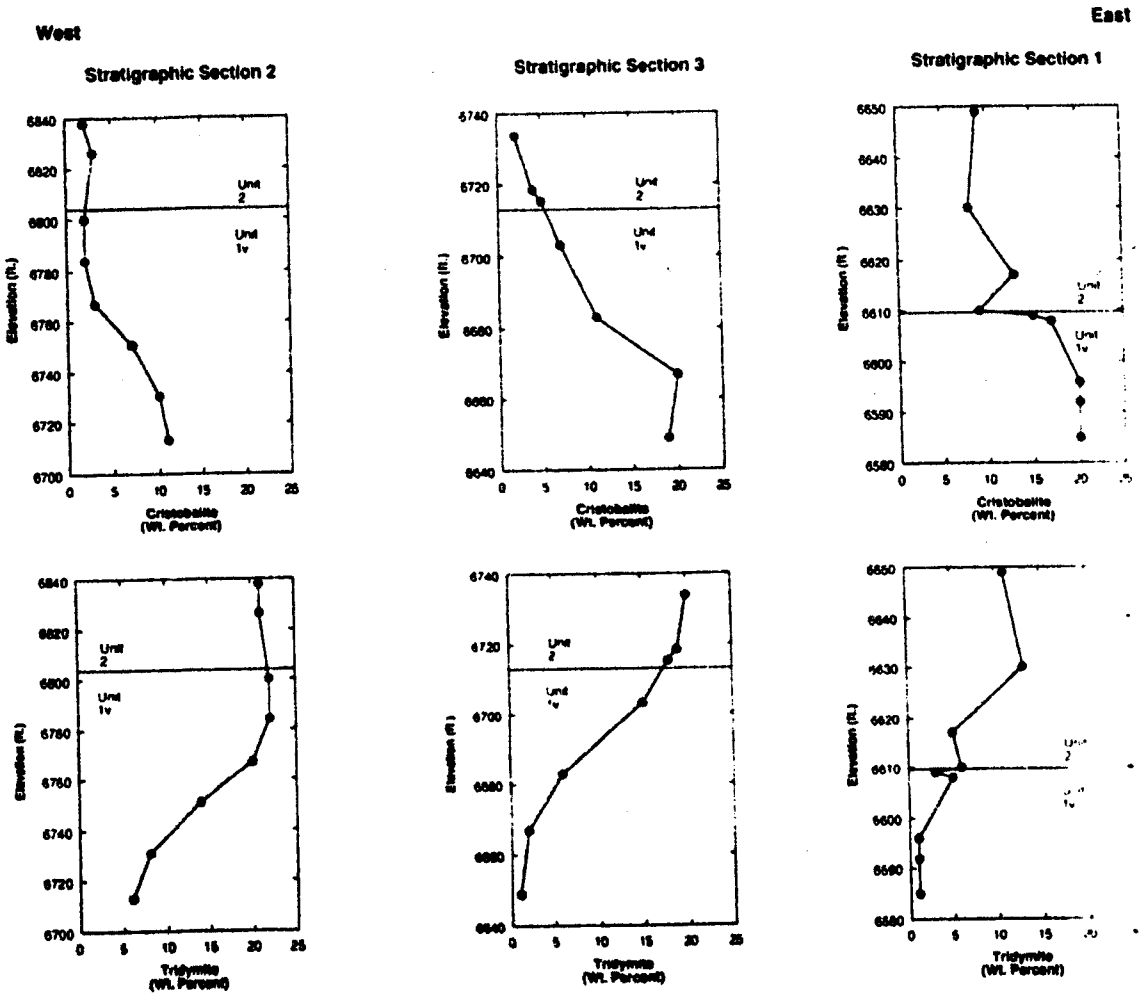

Fig. 6 Variation diagrams showing the abundances of the silica polymorphs tridymite and cristobalite. The abundances of these minerals vary as a function of stratigraphic position and as a function of east-west position at Mesita del Buey. Tridymite and cristobalite abundances vary inversely. In general, greater tridymite abundances are related to increasing degrees of vapor-phase alteration.

Mineralogical data for the measured stratigraphic sections show that tridymite, an indicator mineral for vapor phase alteration, tends to increase in abundance both up section and from east to west in unit 1v (Fig. 6). This suggests that tuffs in the eastern part of Mesita del Buey were subjected to less vapor-phase alteration than equivalent tuffs to the west.

The second hypothesis is supported by variations in chemistry through unit 1. Petrologic studies of the Bandelier Tuff have shown that there are well defined chemical variations in many minor and trace elements in the Bandelier Tuff that reflected the systematic with

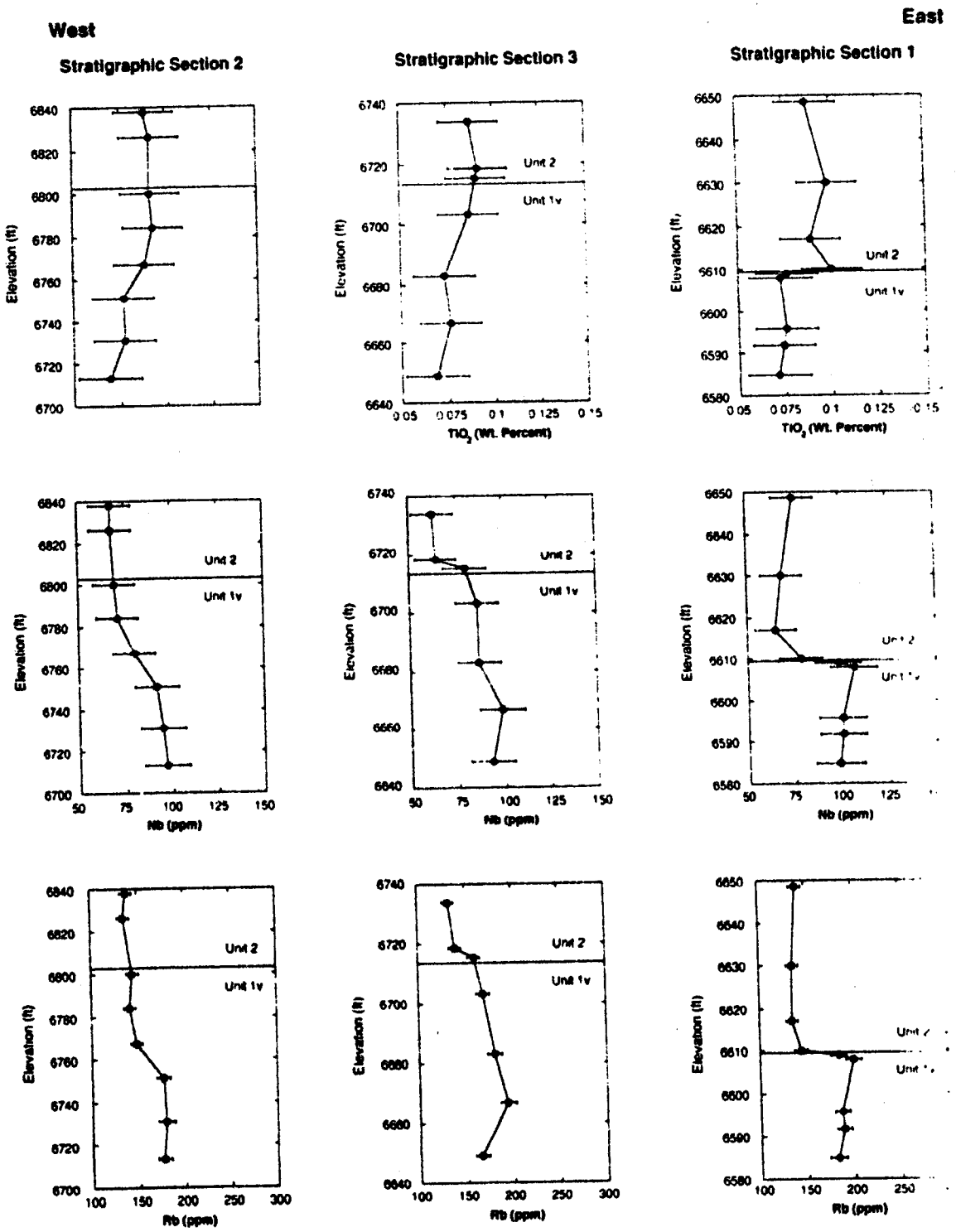

Fig. 7 Variation diagrams showing the variations in Ti, Rb, and Nb as a function of stratigraphic position and east-west position at Mesita del Buey. There is a compositional gap in these trace element abundances across the unit 1v/2 boundary at the east end of Mesita del Buey. This gap disappears to the west, probably reflecting a more complete sequence of Tshirege tuffs closer to their caldera source.

drawal of magma from a chemically-zoned magma chamber (Smith, 1979). Chemical data for the measured sections show that chemical variations from unit 1v and unit 2 form a continuum of compositions in tuffs in the western part of Mesita del Buey, but there is a compositional gap separating the two units in the eastern part (Fig. 7). The most plausible explanation for these data is that a more complete sequence of unit 1v ash flows was deposited in the western part of Mesita del Buey, and nondeposition of some of the same tuffs in the eastern part of mesa resulted in the development of the compositional gap unit 1v/unit 2 boundary.

It is likely that both hypotheses for the thinning of unit 1v eastwards are partially correct. Nondeposition of ash flows in upper unit 1 in the eastern part of the area would result in thinner unit 1 deposits. These thinner deposits would tend to cool more quickly and conditions necessary for the development of a crystallization zone at the top of the unit would be less likely to occur.

Unit 2 Unit 2 is the cliff-forming unit that forms the caprock to Mesita del Buey (Fig. 4). This unit forms medium-brown, near-vertical cliffs that stand out in marked contrast to light-colored, slope-forming tuffs below. Unit 2 is 10 to 15 m thick beneath MDAL and 15 to 20 m

Fig. 8 Photograph of surge deposits at the base of Tshirege Member unit 2. These surge deposits are finely bedded and typically form hump-like deposits that thin laterally. Where absent, the stratigraphic level of the surge deposits is marked by a persistent horizontal parting. As many as three surge deposits occur within the lower 3 m of unit 2. Note the flattening of pumices in the welded tuffs of unit 2 and the equant pumices in nonwelded unit 1v.

thick in the vicinity of MDA G (Fig. 3). The thickness of unit 2 at MDA L is somewhat less than that at MDA G because Mesita del Buey is narrower at MDA L, and more of the upper part of unit 2 has been removed by erosion. In wider mesas to the north and south, where there is more complete preservation of unit 2, these caprock tuffs become thinner eastward. At drill hole SHB-1 at TA-55 (Gardner et al., 1993), unit 2 is about 35 m thick.

Unit 2 is partially to moderately welded and has pumice aspect ratios of 2:1 to 4:1. Unit 2 is significantly less welded than outcrops to the west such as those at Pajarito Mesa (Broxton et al., 1995b) and TA-21 (Broxton et al., 1995a). Nonetheless, unit 2 is more welded than other tuffs at Mesita del Buey. The greater degree of welding in unit 2 has a significant effect on its hydraulic properties relative to underlying units. For example, Rogers and Gallaher (1995)

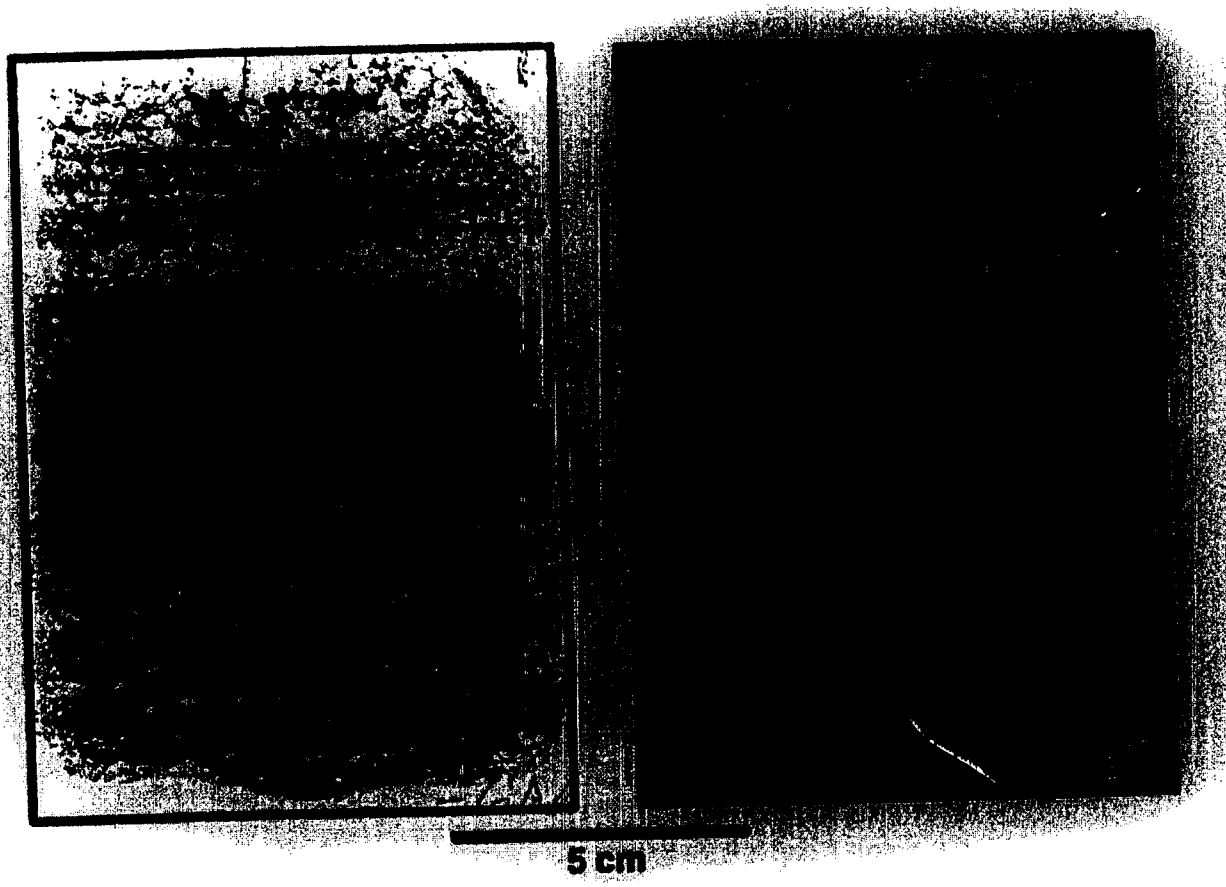

Fig. 9 Photomicrographs of surge bed at the base of unit 2 in stratigraphic section 1, sample 6. Both images are of the same surge bed. The left image is a normal transmitted light image and the right one was generated using crossed polarized light. The slab was cut perpendicular to bedding, mounted on a glass plate, and cut and polished to a 30-micron thickness. The top of the surge bed is oriented up.Stratification in this surge deposit is due to alternating crystal-rich layers (white grains on left image and white, gray, and yellow grains on right image) and ash-rich layers (brown areas in left image). Crystal-rich zones are best developed in the upper part of this surge deposit. The proportions of crystals to ash varies greatly in the surge deposits at Mesita del Buey.

show that saturated conductivity for unit 2 is significantly less than that found in unit 1v. This suggests that travel times of water and vapor by porous matrix flow will be slower in unit 2 relative to underlying units.

However, because of its greater degree of welding, unit 2 is more brittle than underlying tuffs and it typically is more highly fractured. These fractures provide possible fast paths for movement of water and vapor. Most fractures are nearly vertical although some horizontal and low-angle fractures are also present. Many of the fractures extend into the upper part of unit 1v before dying out. Near-surface fractures typically are filled by clays, tuff detritus, and calcite. In borehole 54-1006 near MDA L, some fractures contain small El Cajeta pumice fragments 10 m below the present-day land surface (Caporuscio, 1994). The occurrence of El Cajeta pumice fragments in fractures at depth indicates that some fractures are transport pathways for surface-derived materials.

Unit 2 is characterized by medium-gray to gray-brown crystal-rich pumice relicts supported by an ashy matrix of shards, pumice fragments, and abundant phenocrysts. The matrix is light pink-tan to purple-gray and tends to be more highly colored in the zones of greatest welding. Pumices are generally smaller (<2 cm) and less abundant (2-15%) than in underlying tuffs, except for local pumice swarms which occur in the lower part of the unit. Devitrification and vapor-phase crystallization have destroyed most of the primary vitroclastic textures in the tuff. In hand specimens, relict pumices have a sugary texture due to the deposition of tridymite and sanidine in open pore spaces. Phenocrysts are more abundant (17 to 32%, Broxton et al., 1995a,b) than in unit 1, in part because of the lower porosities in these more-compacted tuffs.

Unit 2 contains several surge beds within 1-3 m of the base of the unit. In addition, two surge deposits were found in the upper part of the unit at Pit 39. The surge beds commonly range in thickness from 0.5 to 6 cm. The thickest surge deposit found is 50 cm thick and crops out on the north wall of Canada del Buey. The surge beds form hump-like deposits which thin to feather edges (Fig. 8). Laterally, these surge deposits are discontinuous, and they grade into horizontal partings that separate thin, nonwelded pumiceous ash-flow tuffs. Up to three surge deposits occur at the base of the unit at some locations.

The surge deposits form planar and cross-bedded dunes. Stratification is imparted by numerous, thin, alternating beds of crystals and ash-rich tuff (Fig. 8). The crystal-rich layers are made up almost entirely of phenocrysts which have been highly concentrated by emplacement processes. Individual layers within the surge deposits are a few millimeters to 3 centimeters thick (Fig. 9).

In some areas, the presence of nonwelded pumice-rich ash-flow tuffs at the base of unit 2 can cause confusion when assigning the lower contact of the unit. These tuffs are very similar to those at the top of unit 1v. The nonwelded pumice-rich tuffs at the base of unit 2 represent the distal ends of small ash flows which pinch out eastwards. If traced westward, towards their source areas, these thin pumice-rich tuffs thicken and grade laterally into partially-welded pumice-poor deposits that are more typical of unit 2. Therefore, for mapping purposes, the base of unit 2 is defined as the base of the lowermost persistent surge deposit or its equivalent parting at the base of the unit 2 cliff. However, because of the poor preservation of surge deposits in drill core, it is recommended the unit 2/unit 1v contact be defined as the ch[illegible]

TABLE II.

MINERALOGY OF TUFFS AT MESITA DEL BUEY, LOS ALAMOS, NEW MEXICO[1]

Sample Number	Strat. Unit[2]	Elevation (ft)	Tridymite	Cristobalite	Quartz	Feldspar	Hematite	Hornblende	Mica	Smectite	Total
Stratigraphic Section 1											
OU-1148-STRAT1-1	Qbt-1v	6585.0	1 ± 1	20 ± 2	16 ± 1	59 ± 8	Tr	Tr	—	—	96 ± 8
OU-1148-STRAT1-2	Qbt-1v	6592.0	1 ± 1	20 ± 2	16 ± 1	58 ± 8	Tr.	1 ± 1	—	—	96 ± 8
OU-1148-STRAT1-3	Qbt-1v	6596.0	1 ± 1	20 ± 2	17 ± 1	57 ± 8	Tr.	Tr	—	—	95 ± 8
OU-1148-STRAT1-4	Qbt-1v	6608.0	5 ± 1	17 ± 1	16 ± 1	60 ± 8	1 ± 1	Tr	—	—	99 ± 8
OU-1148-STRAT1-5	Qbt-1v	6609.0	3 ± 1	15 ± 1	20 ± 2	59 ± 8	1 ± 1	—	—	—	98 ± 8
OU-1148-STRAT1-6	Qbt-2 (surge)	6610.0	6 ± 1	9 ± 3	23 ± 2	61 ± 9	1 ± 1	Tr	—	—	100 ± 10
OU-1148-STRAT1-7	Qbt-2	6617.0	5 ± 1	13 ± 1	19 ± 1	62 ± 9	1 ± 1	—	—	—	100 ± 9
OU-1148-STRAT1-8	Qbt-2	6630.0	13 ± 1	8 ± 3	14 ± 1	59 ± 8	1 ± 1	Tr	—	—	95 ± 9
OU-1148-STRAT1-9	Qbt-2	6649.0	11 ± 1	9 ± 4	18 ± 1	59 ± 8	1 ± 1	—	—	—	98 ± 9
Stratigraphic Section 2											
OU-1148-STRAT2-1	Qbt-1v	6713.2	6 ± 1	11 ± 1	19 ± 1	58 ± 8	1 ± 1	—	—	—	95 ± 8
OU-1148-STRAT2-2	Qbt-1v	6730.8	8 ± 1	10 ± 1	22 ± 2	59 ± 8	1 ± 1	—	—	—	100 ± 8
OU-1148-STRAT2-3	Qbt-1v	6751.2	14 ± 1	7 ± 3	21 ± 2	59 ± 8	1 ± 1	—	—	—	102 ± 9
OU-1148-STRAT2-4	Qbt-1v	6767.2	20 ± 2	3 ± 1	21 ± 2	59 ± 8	Tr.	Tr.	—	—	103 ± 9
OU-1148-STRAT2-5	Qbt-1v	6784.0	22 ± 2	2 ± 1	18 ± 1	59 ± 8	Tr.	Tr.	—	—	101 ± 8
OU-1148-STRAT2-6	Qbt-1v	6800.0	22 ± 2	2 ± 1	18 ± 1	61 ± 9	Tr	—	—	—	103 ± 9
OU-1148-STRAT2-7	Qbt-2	6826.2	21 ± 2	3 ± 1	16 ± 1	58 ± 8	—	—	—	—	98 ± 9
OU-1148-STRAT2-8	Qbt-2	6838.0	21 ± 2	2 ± 1	16 ± 1	62 ± 9	Tr	—	—	—	101 ± 9
Stratigraphic Section 3											
OU-1148-STRAT3-1	Qbt-1v	6649.0	1 ± 1	19 ± 1	22 ± 2	54 ± 8	Tr	Tr	—	—	[illegible]
OU-1148-STRAT3-2	Qbt-1v	6666.9	2 ± 1	20 ± 2	18 ± 1	57 ± 8	Tr	Tr	—	—	[illegible]
OU-1148-STRAT3-3	Qbt-1v	6683.0	6 ± 1	11 ± 1	20 ± 2	59 ± 8	—	Tr	—	—	[illegible]
OU-1148-STRAT3-4	Qbt-1v	6703.3	15 ± 2	7 ± 3	16 ± 1	57 ± 8	—	—	—	—	[illegible]
OU-1148-STRAT3-5	Qbt-1v	6715.2	18 ± 2	5 ± 2	19 ± 1	58 ± 8	—	Tr.	—	—	[illegible]
OU-1148-STRAT3-6	Qbt-2	6718.4	19 ± 2	4 ± 2	16 ± 1	58 ± 8	1 ± 1	—	—	—	[illegible]
OU-1148-STRAT3-7	Qbt-2	6733.9	20 ± 2	2 ± 1	17 ± 1	56 ± 8	1 ± 1	—	—	—	[illegible]
Stratigraphic Section 5											
OU-1148-STRAT5-1	Qbt-1v	6749.0	7 ± 1	10 ± 1	19 ± 1	59 ± 8	—	—	—	—	[illegible]
OU-1148-STRAT5-2	Qbt-1v	6764.0	13 ± 1	7 ± 3	19 ± 1	59 ± 8	—	Tr	—	—	[illegible]
OU-1148-STRAT5-3	Qbt-1v	6781.0	22 ± 2	2 ± 1	12 ± 1	64 ± 9	2 ± 1	1 ± 1	1 ± 1	—	[illegible]
OU-1148-STRAT5-4	Qbt-1v	6797.0	21 ± 2	2 ± 1	18 ± 1	60 ± 8	1 ± 1	—	—	—	[illegible]
OU-1148-STRAT5-5	Qbt-1v	6813.0	21 ± 2	2 ± 1	21 ± 2	57 ± 8	1 ± 1	—	—	—	[illegible]
OU-1148-STRAT5-6	Qbt-2	6830.0	23 ± 2	2 ± 1	19 ± 1	60 ± 8	1 ± 1	—	—	Tr.	[illegible]
OU-1148-STRAT5-7	Qbt-2	6845.0	23 ± 2	1 ± 1	18 ± 1	60 ± 8	1 ± 1	—	—	—	[illegible]
Stratigraphic Section 6											
OU-1148-STRAT6-1	Qbt-1v	6664.0	1 ± 1	19 ± 1	21 ± 2	56 ± 8	1 ± 1	—	—	—	[illegible]
OU-1148-STRAT6-2	Qbt-1v	6680.0	1 ± 1	20 ± 2	19 ± 1	59 ± 8	—	Tr	—	Tr	[illegible]
OU-1148-STRAT6-3	Qbt-1v	6697.0	7 ± 1	12 ± 1	18 ± 1	59 ± 8	—	—	—	—	[illegible]
OU-1148-STRAT6-4	Qbt-1v	6712.0	12 ± 1	10 ± 1	19 ± 1	62 ± 9	—	Tr.	Tr	—	[illegible]
OU-1148-STRAT6-5	Qbt-2	6726.0	21 ± 2	2 ± 1	20 ± 2	59 ± 8	—	—	—	Tr	[illegible]
OU-1148-STRAT6-6	Qbt-2	6743.0	21 ± 2	2 ± 1	16 ± 1	58 ± 8	1 ± 1	—	—	—	[illegible]
OU-1148-STRAT6-7	Qbt-2	6765.0	23 ± 2	2 ± 1	16 ± 1	62 ± 9	1 ± 1	Tr	—	Tr	[illegible]

[1] *Mineral abundances reported as weight percent; uncertainties are two standard deviation estimates of analytical pre[illegible]*
— indicates mineral not detected; Tr = trace abundance (<0.5 wt. %).
[2] *Strat. Unit - Qbt-1v = Tshirege unit 1v; Qbt-2 = Tshirege unit 2.*

from welded tuffs to nonwelded tuffs in borehole studies. Although different criteria are recommended for surface and borehole studies, these guidelines allow placement of the unit 2/ unit 1v contact to within approximately 2 m.

Mineralogy

The bulk-tuff mineralogy for units 1v and 2 is relatively simple, consisting primarily of alkali feldspar (~60% by weight) and of combinations of three silica polymorphs (tridymite, quartz, and cristobalite). Together, these four minerals make up over 95% of the tuffs (Table II). Alkali feldspar and cristobalite occur mainly in the tuff matrix as fine-grained (micron-size), high temperature devitrification products that replaced the original volcanic glass during cooling of the tuff. The tridymite and some alkali feldspar were deposited in open pore spaces by vapors released during outgassing of the tuff after emplacement. Between 50% and 100% of the quartz and about 25% of the alkali feldspar detected by x-ray diffraction in these tuffs are coarse-grained (1-3 mm) phenocrysts that grew in the magma chamber prior to eruption (Broxton et al., 1995b). Minor constituents in these tuffs include smectite, hematite, hornblende, and mica (Table II).

Alkali feldspar and silica minerals are relatively resistant to mineralogic transformation under present-day geochemical conditons and should remain stable beyond the 10,000-year period being studied for the MDA G performance assessment. These minerals have relatively poor ion-exchange properties and probably provide little in the way of natural mineralogic barriers to contaminant migration. On the other hand, the surfaces of of these minerals have high affinities (Kds > 1000 ml/g) for elements such as Am, Cm, Nb, REE, Sn, Th, Zr, and Pu (Allard et al., 1982; Beall and Allard, 1981; Thomas, 1987; Brandberg and Skagius, 1991, Meijer, 1992), and they may provide retardation by surface complexation.

Smectite and hematite are potentially important trace minerals because they are sorptive of certain radionuclides and could provide important natural barriers to their migration. Smectites are highly selective for cationic radionuclides (Grim, 1968). Magnetite and its alteration products such as hematite have an affinity for uranium and actinide species through surface-complexation (Hsi and Langmuir, 1985; Ho and Miller, 1986; Allard and Beall, 1979; Beall and Allard, 1981; and Allard et al., 1982). Although these minerals occur in small quantities, they are disseminated throughout the stratigraphic sequence and may provide significant retardation potential over long ground water flow paths.

Although not analyzed by x-ray diffraction, thin-section investigations show that unit 1g, the Tsankawi Pumice Bed, and the exposed portion of the Cerro Toledo interval contain large amounts of volcanic glass. These units commonly contain 60 to 80% glass at TA-21 (Broxton et al., 1995a), and they probably contain similar amounts at Mesita del Buey. The glass occurs in pumices and the shardy tuff matrix. The presence of abundant glass and paucity of low temperature alteration minerals such as smectites and zeolites indicates that these tuffs have had limited contact with groundwater since their deposition.

The abundances of the silica minerals in units 1v and 2 vary as a function of stratigraphic position as well as distance from the source caldera. Figure 6 shows cristobalite and tridymite abundances plotted versus stratigraphic height for the three stratigraphic sections in Pajarito

Canyon. Tridymite abundances are greatest in unit 2 and in the upper part of unit 1v in the westernmost section. Further east, tridymite abundances decrease overall, and tridymite is most abundant in unit 2. Cristobalite abundances vary inversely with respect to tridymite, suggesting the occurrence of these minerals is controlled by coupled processes. Tridymite is an indicator mineral for vapor-phase alteration and its abundance in unit 2 suggests that post-emplacement vapor phase activity was greater in the upper tuffs at Mesita del Buey. The decrease in tridymite abundances coupled with the thinning of units suggest that vapor phase activity decreased eastward in the distal parts of these tuffs.

Chemistry

Bulk-rock chemical compositions for units 1v and 2 at Mesita del Buey are given in Table III. In addition, two pumice compositions are presented for the Tsankawi Pumice Bed, as discussed below.

The Tshirege Member at Mesita del Buey is made up of high-silica rhyolite (77% SiO_2, on a volatile-free basis). Major element abundances are the same for both units, but some trace element abundances vary with stratigraphic height (Table III and Smith, 1979. A compositional gap occurs at the unit 1v/unit 2 contact in the eastern part of the study area (Fig. 7). However, further to the west, there is a compositional continuum across the same contact.

Although dominated by high-silica rhyolite, the Tshirege Member also contains pumice lumps of hornblende dacite (68-70% SiO_2, on a volatile-free basis). Table III presents compositions for a high-silica rhyolite pumice (sample 1148-4-2A) and a hornblende dacite pumice (sample 1148-4-2B) from the same outcrop of the Tsankawi Pumice Bed for comparison. The hornblende pumice lumps make up <2% of the Tshirege Member, and they are found at all stratigraphic levels. Although co-erupted with the high-silica rhyolite, the hornblende pumices represent a magma that was compositionally distinct from the dominant rhyolitic magma of the Bandelier system.

When establishing background chemistry for the site, it must be recognized that background elemental concentrations can vary as a function of stratigraphic position, particularly for trace metals. However, the differences between background elemental concentrations for units 1v and 2 is relatively small for many elements. Where trace element differences are relatively small, a single background value can be used to represent the two units as long as the variability in elemental abundances is well constrained. Also, care must be taken not to over represent the compositions of the hornblende pumice by the selective sampling of single large pumices when establishing the background chemistry of the tuffs.

The chemical data can be used to establish stratigraphic relations in the eastern part of the study because a compositional gap provides a means for locating the unit 1v/2 contact (Fig. 7). This compositional gap may be useful for interpreting subsurface data from characterization boreholes and for selection of instrument locations in monitoring wells targeting the unit 1v/2 contact. In the western part of Mesita del Buey, chemical data can not be used to constrain stratigraphic relations because the depositional record for the Tshirege Member is more complete and there is no compositional gap at the unit 1v/2 contact.

TABLE III.

CHEMICAL ANALYSES OF ASH-FLOW TUFFS AT MESITA DEL BUEY, LOS ALAMOS, NEW MEXICO[1]

Stratigraphic Section OU-1148-STRAT1									
Sample Number	1148-1-1	1148-1-2	1148-1-3	1148-1-4	1148-1-5	1148-1-6	1148-1-7	1148-1-8	1148-1-9
Stratigraphic Unit	Qbt-1v	Qbt-1v	Qbt-1v	Qbt-1v	Qbt-1v	Qbt-2	Qbt-2	Qbt-2	Qbt-2
Location ID	54-6900	54-6901	54-6902	54-6903	54-6904	54-6905	54-6906	54-6907	54-6908
XRF file	BRO263	BRO263	BRO263	BRO263	BRO263	BRO263	BRO263	BRO263	BRO263
Fusion #	4930	4931	4932	4933	4934	4935	4936	4937	4938
Major Elements (wt. %)									
SiO_2	76.0 ± 1.2	76.9 ± 1.1	77.5 ± 1.2	77.5 ± 1.2	76.7 ± 1.1	76.6 ± 1.1	77.0 ± 1.1	77.2 ± 1.2	77.2 ± 1.2
TiO_2	0.07 ± 0.02	0.07 ± 0.02	0.08 ± 0.02	0.07 ± 0.02	0.08 ± 0.02	0.10 ± 0.02	0.09 ± 0.02	0.10 ± 0.02	0.09 ± 0.02
Al_2O_3	11.6 ± 0.3	11.5 ± 0.3	11.9 ± 0.2	11.6 ± 0.3	11.8 ± 0.2	12.0 ± 0.2	11.7 ± 0.2	11.8 ± 0.2	11.6 ± 0.2
Fe_2O_3 (total)	1.49 ± 0.06	1.49 ± 0.08	1.47 ± 0.06	1.42 ± 0.06	1.48 ± 0.06	1.81 ± 0.06	1.42 ± 0.06	1.53 ± 0.06	1.44 ± 0.06
MnO	0.08 ± 0.01	0.08 ± 0.01	0.07 ± 0.01	0.07 ± 0.01	0.07 ± 0.01	0.08 ± 0.01	0.06 ± 0.01	0.06 ± 0.01	0.06 ± 0.01
MgO	<0.09	<0.09	<0.09	<0.09	<0.09	<0.09	<0.09	<0.09	<0.09
CaO	0.39 ± 0.07	0.30 ± 0.07	0.18 ± 0.07	0.24 ± 0.07	0.29 ± 0.07	0.45 ± 0.07	0.34 ± 0.07	0.30 ± 0.07	0.20 ± 0.07
Na_2O	4.29 ± 0.09	4.11 ± 0.07	4.09 ± 0.07	4.22 ± 0.08	4.19 ± 0.07	4.24 ± 0.08	4.15 ± 0.07	3.99 ± 0.07	4.14 ± 0.07
K_2O	4.55 ± 0.05	4.38 ± 0.05	4.42 ± 0.05	4.34 ± 0.04	4.41 ± 0.05	4.44 ± 0.05	4.48 ± 0.05	4.40 ± 0.05	4.45 ± 0.05
P_2O_5	<0.01	0.08 ± 0.01	<0.01	<0.01	0.01 ± 0.01	0.02 ± 0.01	0.03 ± 0.01	0.16 ± 0.01	<0.01
LOI %	0.80	0.62	0.57	0.46	0.36	0.39	0.34	0.50	0.28
Total	99.1	99.6	100.3	100.0	99.5	99.8	99.6	100.1	99.6
Trace Elements (ppm)									
V	<7	<7	<7	<6	<7	<7	<7	<7	<7
Cr	<9	<9	<9	<9	<9	<9	<9	<9	<9
Ni	<7	<6	<6	<6	<6	<6	<6	<6	<6
Zn	88 ± 12	91 ± 12	84 ± 11	83 ± 11	94 ± 12	90 ± 12	70 ± 10	83 ± 11	66 ± 10
Rb	182 ± 9	189 ± 8	187 ± 8	200 ± 8	185 ± 8	144 ± 6	135 ± 6	136 ± 6	141 ± 6
Sr	15 ± 6	19 ± 6	18 ± 6	14 ± 6	16 ± 6	23 ± 6	19 ± 6	26 ± 6	17 ± 6
Y	87 ± 6	89 ± 5	70 ± 5	81 ± 5	79 ± 5	61 ± 5	52 ± 4	47 ± 4	45 ± 4
Zr	208 ± 15	207 ± 14	199 ± 14	211 ± 14	206 ± 14	196 ± 14	209 ± 14	210 ± 14	215 ± 14
Nb	99 ± 13	100 ± 12	100 ± 12	107 ± 13	98 ± 12	79 ± 12	65 ± 11	69 ± 11	75 ± 11
Ba	60 ± 20	109 ± 16	72 ± 16	35 ± 15	71 ± 16	87 ± 16	82 ± 16	102 ± 16	96 ± 16

[illegible] estimates of analytical precision.

[illegible] Qbt 1g = Tshirege unit 1, lower glassy part, Qbt [illegible]

TABLE III. (CONT)

CHEMICAL ANALYSES OF ASH-FLOW TUFFS AT MESITA DEL BUEY, LOS ALAMOS, NEW MEXICO[1]

Stratigraphic Section OU-1148-STRAT2								
Sample Number	1148-2-1	1148-2-2	1148-2-3	1148-2-4	1148-2-5	1148-2-6	1148-2-7	1148-2-8
Stratigraphic Unit	Qbt-1v	Qbt-1v	Qbt-1v	Qbt-1v	Qbt-1v	Qbt-2	Qbt-2	Qbt-2
Location ID	54-6909	54-6910	54-6911	54-6912	54-6913	54-6914	54-6915	54-6916
XRF file	BRO263	BRO263	BRO263	BRO263	BRO263	BRO263	BRO263	BRO263
Fusion #	4939	4940	4941	4942	4943	4944	4945	4946
Major Elements (wt. %)								
SiO_2	76.8 ± 1.1	77.0 ± 1.2	77.7 ± 1.2	77.3 ± 1.2	77.1 ± 1.1	77.5 ± 1.2	78.5 ± 1.2	77.9 ± 1.2
TiO_2	0.07 ± 0.02	0.08 ± 0.02	0.08 ± 0.02	0.09 ± 0.02	0.09 ± 0.02	0.09 ± 0.02	0.09 ± 0.02	0.09 ± 0.02
Al_2O_3	11.5 ± 0.3	11.7 ± 0.3	11.8 ± 0.2	11.6 ± 0.3	11.6 ± 0.3	11.8 ± 0.2	11.7 ± 0.2	12.1 ± 0.2
Fe_2O_3 (total)	1.43 ± 0.06	1.52 ± 0.06	1.46 ± 0.06	1.47 ± 0.06	1.47 ± 0.06	1.48 ± 0.06	1.46 ± 0.06	1.45 ± 0.06
MnO	0.07 ± 0.01	0.07 ± 0.01	0.07 ± 0.01	0.07 ± 0.01	0.06 ± 0.01	0.06 ± 0.01	0.06 ± 0.01	0.06 ± 0.01
MgO	<0.09	<0.09	<0.09	<0.09	<0.09	<0.09	<0.09	<0.09
CaO	0.26 ± 0.07	0.26 ± 0.07	0.27 ± 0.07	0.38 ± 0.07	0.35 ± 0.07	0.23 ± 0.44	0.23 ± 0.07	0.21 ± 0.07
Na_2O	4.16 ± 0.07	4.13 ± 0.08	4.08 ± 0.07	4.08 ± 0.07	4.09 ± 0.07	4.07 ± 0.07	3.98 ± 0.07	4.13 ± 0.07
K_2O	4.28 ± 0.04	4.36 ± 0.05	4.38 ± 0.05	4.33 ± 0.04	4.28 ± 0.04	4.36 ± 0.05	4.37 ± 0.05	4.58 ± 0.05
P_2O_5	<0.01	<0.01	0.03 ± 0.01	0.05 ± 0.01	0.02 ± 0.01	0.01 ± 0.01	<0.01	<0.01
LOI %	0.52	0.30	0.29	0.34	0.24	0.28	0.37	0.36
Total	99.1	99.4	100.1	99.6	99.2	99.9	100.9	100.9
Trace Elements (ppm)								
V	<6	<7	<7	<7	<7	<7	<7	<7
Cr	<9	<9	<9	<9	<9	<9	<9	<9
Ni	<6	<7	<6	<6	<6	<6	<6	<6
Zn	81 ± 11	91 ± 12	73 ± 11	71 ± 11	80 ± 11	72 ±	67 ± 10	83 ± 11
Rb	177 ± 8	180 ± 9	177 ± 7	148 ± 7	141 ± 6	144 ±	135 ± 6	138 ± 6
Sr	14 ± 6	20 ± 6	17 ± 6	26 ± 6	29 ± 6	24 ± 6	20 ± 6	18 ± 6
Y	79 ± 5	80 ± 6	70 ± 5	59 ± 5	61 ± 5	55 ± 5	32 ± 4	47 ± 4
Zr	196 ± 14	200 ± 15	208 ± 14	203 ± 14	204 ± 14	207 ± 14	215 ± 14	212 ± 14
Nb	97 ± 12	95 ± 12	92 ± 12	80 ± 12	71 ± 11	69 ± 11	67 ± 11	68 ± 11
Ba	[illegible]	[illegible]	[illegible]	[illegible]	116 ± 16	102 ± 16	85 ± 16	100 ± 16

TABLE III. (CONT)

CHEMICAL ANALYSES OF ASH-FLOW TUFFS AT MESITA DEL BUEY, LOS ALAMOS, NEW MEXICO[1].

	Stratigraphic Section QU-1148-STRAT3							Stratigraphic Section QU-1148-STRAT4		
Sample Number	1148-3-1	1148-3-2	1148-3-3	1148-3-4	1148-3-5	1148-3-6	1148-3-7	1148-4-2A	1148-4-2B	1148-4-3
Stratigraphic Unit	Qbt-1v	Qbt-1v	Qbt-1v	Qbt-1v	Qbt-1v	Qbt 2	Qbt-2	Qbt-1(r)	Qbt-1(d)	Qbt-1g
Location ID	54-6917	54-6918	54-6919	54-6920	54-6921	54-6922	54-6923	54-6925	54-6926	54-6927
XRF file	BRO263	BRO263	BRO263	BRO263	BRO263	BRO266	BRO266	BRO261	BRO261	BRO266
Fusion #	4947	4948	4949	4950	4951	4952	4953	4970	4971	4954
Major Elements (wt. %)										
SiO_2	75.9 ± 1.1	77.5 ± 1.2	77.5 ± 1.2	77.5 ± 1.2	77.7 ± 1.2	76.3 ± 1.1	77.8 ± 1.2	74.7 ± 1.1	68.2 ± 1.0	77.4 ± 1.2
TiO_2	0.07 ± 0.02	0.08 ± 0.02	0.07 ± 0.02	0.09 ± 0.02	0.09 ± 0.02	0.09 ± 0.02	0.09 ± 0.02	0.06 ± 0.02	0.41 ± 0.01	0.07 ± 0.02
Al_2O_3	11.4 ± 0.3	11.7 ± 0.2	11.6 ± 0.3	11.8 ± 0.2	11.7 ± 0.2	11.9 ± 0.2	12.1 ± 0.2	11.8 ± 0.2	14.3 ± 0.2	11.5 ± 0.3
Fe_2O_3 (total)	1.35 ± 0.06	1.46 ± 0.06	1.44 ± 0.06	1.52 ± 0.06	1.49 ± 0.06	1.46 ± 0.06	1.43 ± 0.06	1.68 ± 0.06	3.28 ± 0.07	1.45 ± 0.06
MnO	0.07 ± 0.01	0.07 ± 0.01	0.07 ± 0.01	0.06 ± 0.01	0.07 ± 0.01	0.06 ± 0.01	0.06 ± 0.01	0.09 ± 0.01	0.07 ± 0.01	0.07 ±
MgO	0.16 ± 0.09	<0.09	<0.09	<0.09	<0.09	<0.09	<0.09	<0.09	1.15 ± 0.07	<0.09
CaO	0.74 ± 0.08	0.32 ± 0.07	0.31 ± 0.07	0.23 ± 0.07	0.48 ± 0.07	0.20 ± 0.07	0.22 ± 0.07	0.34 ± 0.07	2.70 ± 0.07	0.38 ± 0.07
Na_2O	4.20 ± 0.07	4.15 ± 0.07	4.19 ± 0.07	4.24 ± 0.08	4.13 ± 0.07	4.17 ± 0.07	3.99 ± 0.07	4.21 ± 0.08	4.97 ± 0.11	3.70 ± 0.06
K_2O	4.43 ± 0.05	4.28 ± 0.04	4.29 ± 0.04	4.40 ± 0.05	4.35 ± 0.05	4.47 ± 0.05	4.54 ± 0.05	4.38 ± 0.05	3.18 ± 0.04	4.52 ± 0.05
P_2O_5	<0.01	<0.01	<0.01	<0.01	0.02 ± 0.01	<0.01	0.03 ± 0.01	<0.01	0.14 ± 0.01	<0.01
LOI %	1.73	0.50	0.34	0.52	0.52	0.31	0.52	3.16	2.40	1.43
Total	100.0	100.0	99.8	100.4	100.5	99.0	100.7	100.4	100.8	100.5
Trace Elements (ppm)										
V	<6	<7	<7	<7	<7	<7	<7	<6	33 ± 10	<6
Cr	<9	<9	<9	<9	<9	<9	<9	<9	17 ± 9	<9
Ni	<6	<6	<6	<6	<6	<6	<6	<6	<7	<6
Zn	79 ± 11	89 ± 12	101 ± 12	91 ± 12	88 ± 12	70 ± 10	62 ± 10	147 ± 16	68 ± 10	100 ± 12
Rb	165 ± 7	194 ± 8	180 ± 8	168 ± 7	159 ± 7	139 ± 6	133 ± 6	295 ± 11	186 ± 8	224 ± 9
Sr	25 ± 6	19 ± 6	17 ± 6	21 ± 6	24 ± 6	22 ± 6	23 ± 6	15 ± 6	368 ± 8	13 ± 6
Y	79 ± 5	79 ± 5	69 ± 5	65 ± 5	74 ± 5	62 ± 5	48 ± 4	113 ± 7	35 ± 6	81 ± 6
Zr	193 ± 14	207 ± 14	190 ± 14	204 ± 14	212 ± 14	209 ± 14	211 ± 14	266 ± 16	205 ± 15	200 ± 14
Nb	93 ± 12	99 ± 12	87 ± 12	86 ± 12	80 ± 12	64 ± 11	63 ± 11	165 ± 15	31 ± 10	103 ± 12
Ba	62 ± 16	69 ± 16	72 ± 16	73 ± 16	80 ± 15	109 ± 16	108 ± 16	78 ± 15	748 ± 28	64 ± 16

CONCLUSIONS

The Tshirege Member of the Bandelier Tuff is a multiple-flow ash-flow sheet that forms prominent cliffs and benches at Pajarito Canyon, Mesita del Buey, and Canada del Buey. It is a compound cooling unit whose physical properties vary both vertically and laterally. These variations in physical properties result from zonal patterns of welding and crystallization.

Exposed bedrock at Mesita del Buey and vicinity consists of, in ascending order: 1) fluvial deposits of the Cerro Toledo interval, 2) the Tsankawi Pumice Bed, 3) unit 1g of the Tshirege Member, 4) unit 1v (including the lower colonnade part and the upper less resistant part), and 5) unit 2 of the Tshirege Member. These units should be treated as separate hydrogeological units during performance assessment because their dissimilar lithologic properties results in significant differences in hydraulic properties. In addition, the geometry of potential vertical transport pathways changes as units of the Bandelier Tuff become thinner eastward.

The bulk-tuff mineralogy of the tuffs at Mesita del Buey consists primarily (>95%) of alkali feldspar, tridymite, quartz, and cristobalite. Alkali feldspar and silica minerals are relatively resistant to transformation and should remain stable over the life time of the MDAs. Smectite and hematite, which occur in small amounts throughout the stratigraphic sequence, are important because they are sorptive of certain radionuclides and could provide important natural barriers to their migration.

The Tshirege Member at Mesita del Buey is a high-silica rhyolite (77% SiO_2). Major element abundances are relatively constant through the unit, but some trace element abundances vary with stratigraphic height. When establishing baseline conditions for the site, it must be recognized that background elemental concentrations for some trace elements can vary as a function of stratigraphic position. The chemical data can be used to establish stratigraphic relations in the eastern part of the study because a compositional gap provides a means for locating the unit 1v/2 contact . This compositional gap may be useful for interpreting subsurface data from characterization boreholes and for selection of instrument locations in monitoring wells. The chemical data can not be used to constrain stratigraphic relations to the west because there is a compositional continuum across the same contact.

ACKNOWLEDGMENTS

Field work for this report was funded by the Environmental Restoration Program of Los Alamos National Laboratory, as part of activities supported by OU-1148 and Framework Studies of the Earth Science Technical Team. Publication of this report was funded by the MDA G Performance Assessment. We thank Don Neeper, Bob Gilkesen, Don Krier, and Eric Vold for their program support. D. Mann and Carlos Montoya prepared thin sections of these tuffs, many of which were difficult to mount and polish.

REFERENCES

Allard, B. and Beall, G. W., 1979, Sorption of Am on geologic media, J. of Environ. Sci. and Health, A14 (6). p. 507-518.

Allard, B., Olofsson U., Torstenfelt, B., Kipasti, H., and Anderson, H., 1982, Sorption of Actinides in well-defined oxidation states on geologic media, in Scientific Basis for Nuclear Waste Management V, Materials Research Society Symposia Proceedings, L. Lutze, Ed. (Materials Research Society, Pittsburgh, Pennsylvania), p. 775-786.

Bailey, R. A., Smith, R. L., and Ross, C. S., 1969, Stratigraphic nomenclature of the volcanic rocks in the Jemez Mountains, New Mexico, U.S. Geol. Survey Bull. 1274-P, 19 p.

Baltz, E. H., Abrahams, J. H., Sr., and Purtymun, W. D., 1963, Preliminary report on geology and hydrology of Mortandad Canyon near Los Alamos, New Mexico, with reference to disposal of liquid low-level radioactive wastes, U.S. Geol. Survey open-file report (Albuquerque, NM), 105 p.

Beall, G. W. and Allard, B., 1981, Sorption of actinides from aqueous solutions under environmental conditions, in Proceedings of a Symposium on Adsorption from Aqueous Solutions, March 24-27, 1980, American Chemical Society Meeting, Division of Colloid and Surface Chemistry (Houston, TX), p. 193-212.

Bish, D. L. and Chipera, S. J., 1988, Problems and solutions in quantitative analysis of complex mixtures by X-ray powder diffraction, in Advances in X-Ray Analysis (Plenum Press, New York, 1988), v. 31, p. 295-308.

Bish, D. L. and Chipera, S. J., 1989, Revised mineralogical summary of Yucca Mountain, Nevada, Los Alamos National Laboratory report LA-11497-MS.

Brandberg, F. and Skagius, K., 1991, Porosity, sorption, and diffusivity data compiled for the SKB 91 Study, SKB-TR-91-16 Kaunbranslesakerhet, Stockholm.

Broxton, D.E., Heiken, G., Chipera, S.J., and Byers, F.M., 1995a, Stratigraphy, petrography, and mineralogy of tuffs at Technical Area 21, Los Alamos National Laboratory, New Mexico, Los Alamos National Laboratory Report LA-12934-MS, in press.

Broxton, D. E., Vaniman, D.T., Byers, F. M. ,Jr., Chipera, S. J., Kluk, E. C., and Warren, R. G., 1995b, Stratigraphy, mineralogy and chemistry of bedrock tuffs at Pajarito Mesa, Los Alamos National Laboratory, New Mexico, Los Alamos National Laboratory Report, in review.

Broxton, D. E. and Reneau, S.L., 1995, Stratigraphic Nomenclature of the Bandelier Tuff for Environmental Restoration Studies at Los Alamos National Laboratory, Los Alamos National Laboratory Report, in review.

Caporuscio, F. A., 1994, Description of rock units in drill core at TA-54, Los Alamos National Laboratory, Letter Report June 27, 1994, 9p.

Chung, F. H., 1974a, Quantitative interpretation of X-ray diffraction patterns of mixtures. I Matrix-flushing method for quantitative multicomponent analysis, J. of App. Crystallography, v. 7, p. 519-525.

Chung, F. H., 1974b, Quantitative interpretation of X-ray diffraction patterns of mixtures. II. Adiabatic principle of X-ray diffraction analysis of mixtures, J. of App. Crystallography, v. 7, p. 526-531.

Criss, J., 1980, Fundamental parameters calculations on a laboratory microcomputer, Adv. X-Ray Analysis, v. 23, p. 93-97.

Crowe, B., Linn, G., Heiken, G., and Bevier, M., 1978, Stratigraphy of the Bandelier Tuff in the Pajarito Plateau, applications to waste management, Los Alamos National Laboratory report LA-7225-MS, 57 p.

Rogers, D.B. and Gallaher, B.M., 1995, Unsaturated hydraulic characteristics of the Bandelier Tuff, Los Alamos National Laboratory Report, in review.

Gardner, J. N., Kolbe, T., and Chang, S., 1993, Geology, drilling, and some hydrologic aspects of Seismic Hazards Program Core Holes, Los Alamos National Laboratory, New Mexico, Los Alamos National Laboratory Report LA-12460-MS, 19 p.

Goff, F., Heiken, G. H., Tamanyu, S., Gardener, J., Self, S., Drake, R., and Shafiqullah, M. 1984, Location of Toledo caldera and formation of the Toledo embayment, Jemez Mountains, New Mexico, EOS Trans., Amer. Geophys. Union, *65*, p. 1145.

Griggs, R. L., 1964, Geology and ground-water resources of the Los Alamos area, New Mexico. U.S. Geol. Survey Water-Supply Paper 1753, 107 p.

Grim, R. E., 1968, Clay Mineralogy, 2nd edition, McGraw-Hill Book Company, New York, 596 p.

Ho, C. H. and Miller, N. H., 1986, Adsorption of uranyl species from bicarbonate solution onto hematite particles, J. Colloid Interface Sci., v. 110, p. 165-171.

Hsi, C-K and Langmuir, 1985, Adsorption of uranyl onto ferric oxyhydroxides: Application of the surface complexation site-binding model, Geochim. Cosmochim. Acta, v.49, p. 1931-1941

Izett, G. A. and Obradovich, J. D., 1994, $^{40}Ar/^{39}Ar$ age constraints for the Jaramillo Normal Subchron and the Matuyama-Brunhes geomagnetic boundary, J. Geophys. Res. 99 (B2), p 2925-2934.

Klug, H. P. and Alexander, L. E., 1974, X-Ray Diffraction Procedures for Polycrystalline and Amorphous Materials, John Wiley & Sons, Inc, New York.

Krier, D. .....need reference for performance assessment document

Longmire, O., Duffy, C., and Reneau, S., 1993, Preliminary Background Elemental Concentrations in Bandelier Tuff and Selected Soils Series, 1993, Los Alamos National Laboratory Letter Report.

Longmire, P., Reneau, S., Watt, P., McFadden, L., Gardner, J., Duffy, C., and Ryti, R., 1995, Natural Background Geochemistry, Geomorphology, and Pedogenesis of Selected Soil Profiles and Bandelier Tuff, Los Alamos, New Mexico, 1995, unpublished draft report for Environmental Restoration Project, Los Alamos National Laboratory, January 1995.

Meijer, A., 1992, Experiments and integration of relevant sorption models, Procs. of DOE/ Site Characterization Project Radionuclide Adsorption Workshop, Los Alamos National Laboratory, Sept. 11-12,1990, Los Alamos National Laboratory Conf. Report LA-12325-C, pp. 9-36.

Reneau, S. L., Kolbe, T. R., Simpson, D. T., Carney, J. S., Gardner, J. N., and Vaniman, D. T., 1995, Surficial materials and structure at Pajarito Mesa, Los Alamos National Laboratory, New Mexico, this report.

Self, S., Goff, F., Gardner, J. N., Wright, J. V., and Kite, W. M., 1986, Explosive rhyolitic volcanism in the Jemez Mountains: vent locations, caldera development, and relation to regional structure, J. Geophys. Res., v.91, no. B2, p. 1779-1798.

Smith, R. L. and Bailey, 1966, The Bandelier Tuff: a study of ash-flow eruption cycles from zoned magma chambers, Bull. Volcanologique, v. 29, p. 83-104.

Smith, R. L., Bailey, R. A., and Ross, C. S., 1970, Geologic map of the Jemez Mountains, New Mexico, U.S. Geol. Survey Map I-571, scale 1:1250000.

Smith, R. L., 1979, Ash flow magmatism, Geol. Soc. America Spec. Paper 180, p. 5-27.

Thomas, K. W., 1987, Summary of sorption measurements performed with Yucca Mountain, Nevada, tuff samples and water from well J-13, Los Alamos National Laboratory Report LA-10969-MS.

Turin, J. A., Benton, L., and Broxton, D., 1994, In-situ measurements of Bandelier Tuff: saturated and unsaturated hydrologic conductivity, Los Alamos National Laboratory Quarterly Environmental Restoration Project Technical Sessions Abstracts, October 19, 1194.

Vaniman, D. T. and Wohletz, K., 1990, Results of geological/fracture studies: TA-55 area, Los Alamos National Laboratory, Geology/Geochemistry Group internal report, EES1-SH90-17 25 p.

Vaniman, D., and Wohletz, K., 1991, Revisions to report EES1-SH90-17: Unpub. Rept. EES1 SH91-12, 2 p.

Weir, J. E. and Purtymun, W. D., 1962, Geology and hydrology of Technical Area 49, Frijoles Mesa, Los Alamos County, New Mexico, U.S. Geol. Survey Admin. Release Report, Albuquerque, NM, 225 p.

APPENDIX A

MEASURED SECTIONS IN PAJARITO CANYON AND CANADA DEL BUEY AND ITS TRIBUTARIES

OU-1148-STRAT1

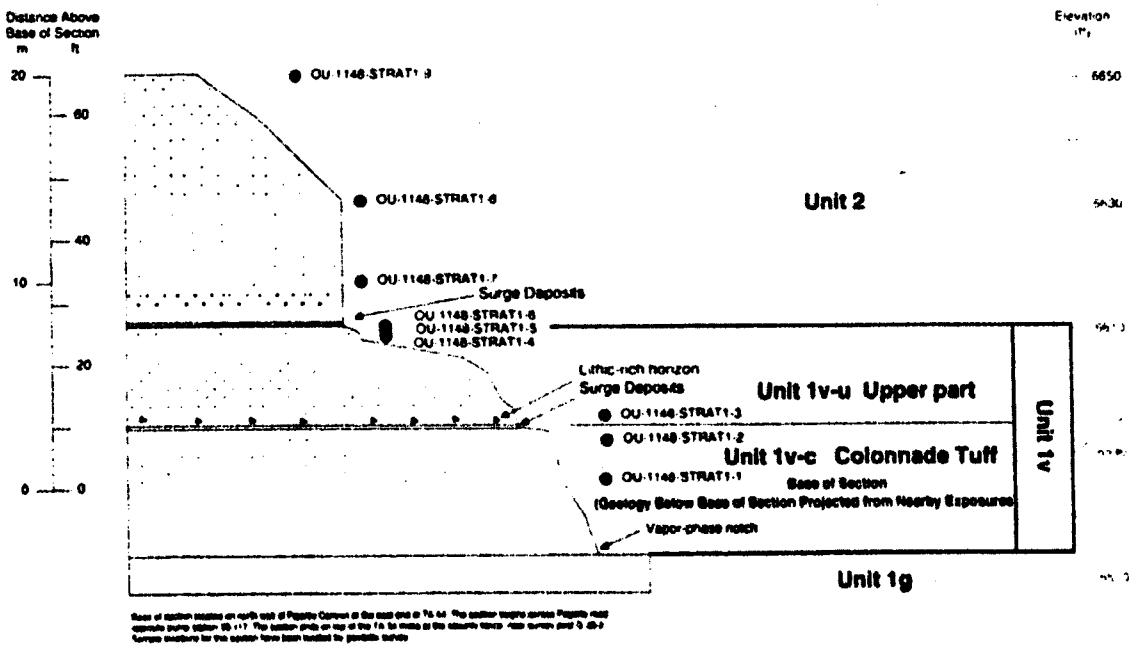

APPENDIX A CONT

OU-1148-STRAT2

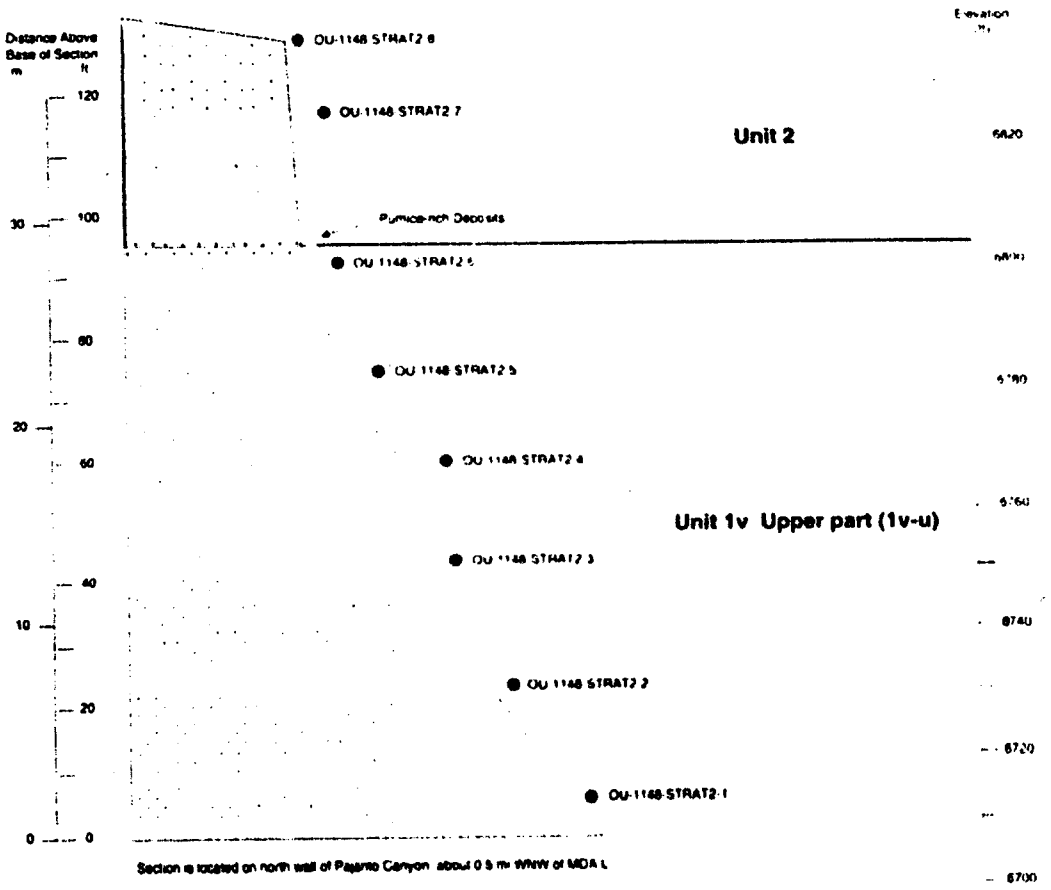

APPENDIX A CONT

OU-1148-STRAT3

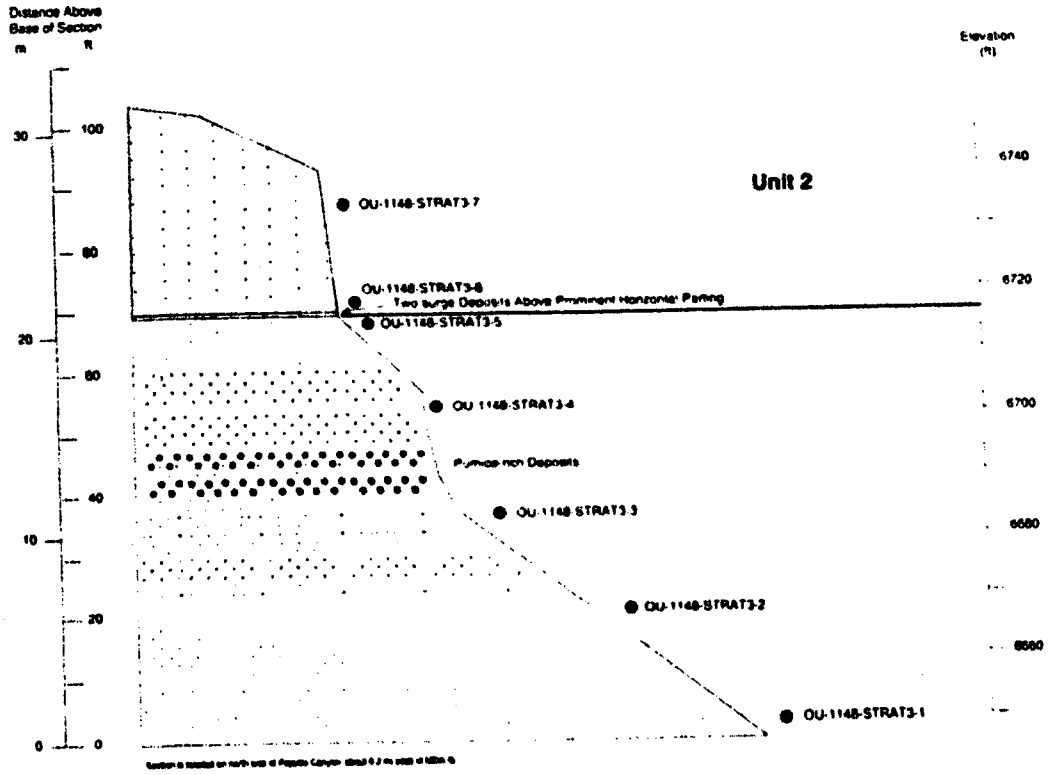

APPENDIX A CONT

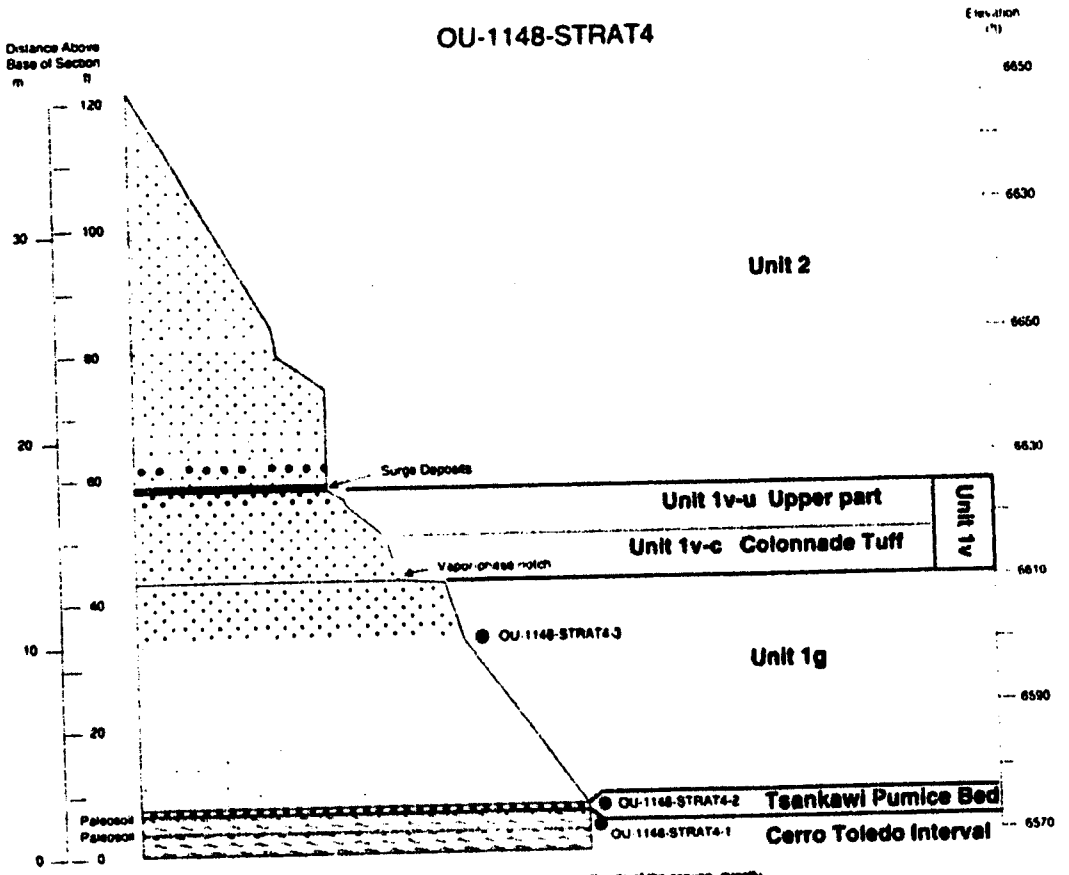

APPENDIX A CONT

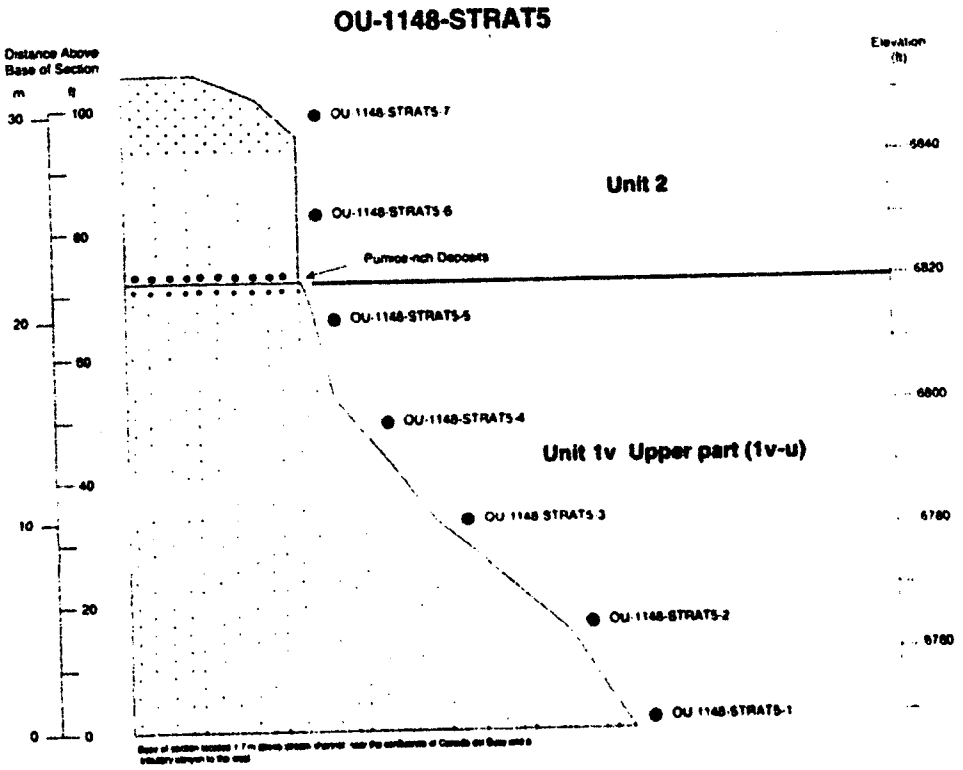
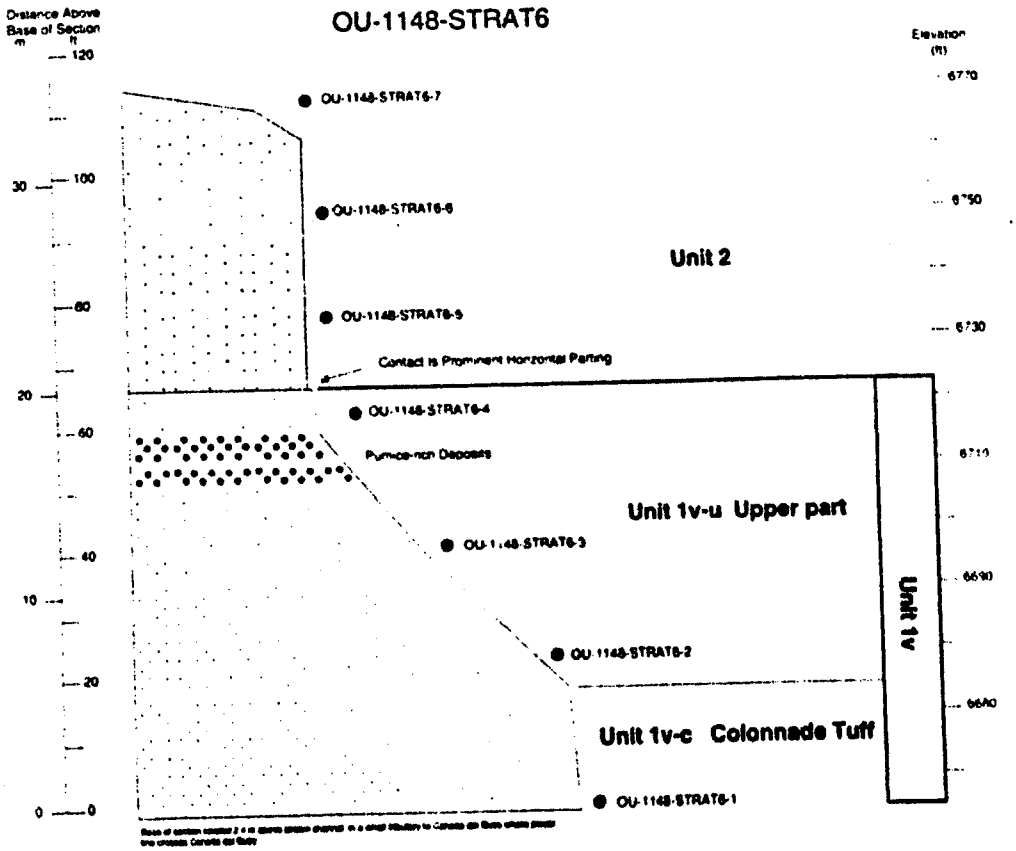
APPENDIX A CONT